SHRP-ID/UFR-92-604

Evaluation of the Use of Laser Ultrasonics for the Rapid, Noncontact Inspection of Concrete and Asphalt

F.K. Brocklehurst
B.C. Moss
R.L. Smith
C.G. Tasker

The National NDT Centre
Harwell Laboratory
Oxfordshire, United Kingdom

Strategic Highway Research Program
National Research Council
Washington, DC 1992

SHRP-ID/UFR-92-604
Contract ID-002

Program Manager: *K. Thirumalai*
Project Managers: *Ataur Bacchus*
Marty Laylor
Program Area Secretary: *Vondell Little*

May 1992

key words:
delamination
laser interferometer
laser ultrasonics
nondestructive evaluation

Strategic Highway Research Program
2101 Constitution Avenue N.W.
Washington, DC 20418

(202) 334-3774

Acknowledgments

The research described herein was supported by the Strategic Highway Research Program (SHRP). SHRP is a unit of the National Research Council that was authorized by section 128 of the Surface Transportation and Uniform Relocation Assistance Act of 1987.

The authors would like to thank Dr. C. Scruby at Harwell for his support and for providing the laser facility.

Contents

List of Figures

List of Tables

Abstract

This report documents the investigation of the use of a laser system for the detection of voids, delaminations, and defects in asphalt and mesh reinforced concrete structures. The goals of the research were to discover whether laser systems could: generate and receive ultrasound in concrete and asphalt; verify that such a system obtains the same information as conventional ultrasonic tests; see if the laser system could obtain more information than conventional tests; and consider how laser ultrasonics would be used in the field.

Executive Summary

This report documents the investigation of the use of a laser system for the detection of voids, delaminations, and defects in asphalt and mesh reinforced concrete structures. The goals of the research were: discover whether laser systems could generate and receive ultrasound in concrete and asphalt; verify that such a system obtains the same information as conventional ultrasonic tests; see if the laser system could obtain more information than conventional tests; and consider how laser ultrasonics would be used in the field.

A pulsed Nd-YAG laser was used to excite the surface of the material with a 75-millijoule, 20-nanosecond pulse. This pulse had a power density of approximately 5 megawatts per square millimeter and produced ultrasonic waves in the sample. A He-Ne laser interferometer of the Michelson type was used to measure the minute movements in the surface of the material caused by the ultrasonic waves. By comparing the phase of the
He-Ne output laser light with the light reflected from the surface of the material, surface movements can be monitored and converted to actual surface displacement values in nanometers.

Three laser beam arrangements were tested: direct transmission; near-coincident; and same surface-separated. In direct transmission, the Nd-YAG laser was fired at one face of the slab and the interferometer was focused on the opposite face. Direct transmission restricts use to locations with access to both the top and bottom surfaces, such as bridges.
The near-coincident arrangement placed the two lasers so that they were nearly focused on the same point on the same surface. This maximized the reflected energy to the interferometer and carried the most information about the compression wave. The near-coincident arrangement had two major drawbacks. The flash of light from the Nd-YAG laser could scatter into the photodiodes of the interferometer, causing interference. Also, an acoustic wave could appear early because of the small separation between the lasers. These disturbances could mask the presence of other useful information, such as the surface and compression wave information.

The laser system was tested on asphalt and portland cement concrete sections 35, 65, 100, 150, 200, and 250 mm thick. A number of the concrete samples had simulated delaminations, and voids. Reinforcing mesh was used in some of the portland cement concrete samples. These samples were used to assess the laser system's ability to detect defects and artifacts in concrete.

Due to the surface texture and poor reflectivness of asphalt and concrete, not much of the incident light reflected back to the interferometer. Reflective paint was tried on the surface to improve reflection. This technique is not feasible in the field, but in the laboratory it meant that research could be conducted without obtaining either a more powerful laser or a more sensitive interferometer.

The waveforms had five prominent features: the firing pulse from the Nd-YAG laser; the surface wave; the reflected compression wave; the reflected shear wave; and the acoustic air wave. This information was used in an attempt to determine the thickness of concrete and the depth of defects in the concrete.

The concrete blocks 100, 150, 200, and 250 mm thick presented no problems in scanning other than the attenuation of the peak from the reflected compression wave as thickness increased. With thicknesses of 200 mm or more, the reflected compression wave was almost indiscernible from the background noise. A more powerful impact laser would overcome this obstacle.

The concrete samples that contained simulated defects produced encouraging results. Delamination showed up as a broad peak superimposed on the general background. Mesh, when present, was not consistently detected. Simulated voids in the samples were detectable.

A lightly wetted surface did not cause problems. However, water deeper than a millimeter dissipated the laser pulse energy greatly.

The test results from asphalt samples were variable. It was difficult to obtain for the compression wave peak from the bottom surface of fresh, hot-rolled asphalt. The surface wave energy diminished quickly because of the rough surface finish. A delamination in an aged asphalt sample taken from the field showed up very well. In general, aged asphalt provided much better results than fresh, hot-rolled asphalt.

This research indicates that laser systems can be used to produce and detect ultrasonic waveforms in asphalt and concrete samples. The ultrasonic responses obtained from the test samples using this system compared favorably with results from inspections performed with conventional ultrasonic equipment. The techniques developed in this research show that compression wave velocity, thickness, and some defects can be measured without physical contact. Much more work in instrument development and signal enhancement, automatic recognition, and processing would be necessary to create a portable prototype.

1. Introduction

This report describes work carried out for the Strategic Highway Research Program. It addresses the specific problem of inspecting concrete and asphalt pavements and also concrete structures non-destructively, through a research program contract, awarded under the S.H.R.P. - I.D.E.A. Program to the National NDT Centre in the U.K. The program investigated the feasibility of developing a non-contacting ultrasonic based system that would offer the ability to inspect large areas of concrete and asphalt rapidly.

It was proposed that such a system should be based upon lasers to generate and detect ultrasonic waves in concrete and asphalt samples using new techniques developed for this purpose. An experimental program was set up with the main objectives being:

- to demonstrate that ultrasound can be generated and received in concrete and asphalt using laser systems;

- to verify that all the information obtainable from conventional ultrasonic tests on concrete, can also be obtained using laser-based probes;

- to evaluate what additional information may be obtained through the use of laser ultrasonics;

- to consider how the inspection of concrete and asphalt by laser ultrasonics might be carried out in practice.

Ultrasonic inspection and characterisation of heterogeneous materials such as concrete and asphalt have generally been performed using piezo-electric transducers of moderately low frequency 25 kHz → 1 MHz. This technique requires the application of a suitable couplant to be used to

maintain good acoustic contact between the material and the transducer face and therefore does not facilitate rapid scanning of large areas for inspection.

However, it has been recognised recently that lasers can provide the basis of a totally non-contacting system for inspecting metals[1] with ultrasound and hence may be the basis of a system for the rapid inspection of large areas of concrete and asphalt as on highways. Nevertheless, there are difficulties associated with this technique of remote generation and detection of ultrasound in concrete and asphalt, due largely to the nature of these materials; they are both highly attenuating to the passage of ultrasound. Sufficient acoustic energy has to be imparted to the material in the first instance to ensure that a reflected wave will remain detectable after travelling through thicknesses of many centimetres. Also, the optical reflectivity and the surface texture of concrete and asphalt are poor and greatly hinder detection by laser interferometer.

Methods of overcoming these difficulties have been explored and the experimental work has been carried out on many samples to determine the capability of such a system to detect defects and artefacts in concrete and asphalt. The main experimental facilities are illustrated in Figure 2.

2. Physical Principles

When a very high power-density laser pulse is directed at the surface of a material such as concrete, a small amount of the material at the impact point is vaporised to a depth of a few micrometres, to a degree dependant upon the absorption of the material. This process is called 'ablation'. It is not a truly non-destructive technique since some damage is caused to the surface of the material, but this is small and its effect negligible on coarse surfaces such as concrete and asphalt. An equally intensive source, which is less damaging to the surface, can be generated if the surface of the target area of

the specimen is thinly coated with a liquid such as water. The concentrated energy in the laser pulse causes the liquid locally to vaporise rapidly sending a pressure pulse into the material.

As shown in Figure 3, the ablation of the material produces three modes of stress wave propagation in that material: longitudinal (compression wave), translational (shear wave) and elliptical (Rayleigh or surface wave). These are often denoted by the abbreviations: P-wave, S-wave and R-wave (see Appendix B). Monitoring of these modes of vibration in the material can reveal information about the properties and structure of the material itself. Generally, high compression wave velocities in concrete are indicative of good quality concrete and conversely, low velocities indicative of poor quality concrete[2]. The compression wave velocity and the shear wave velocity may be used to calculate a value for Poisson's ratio (approximately 0.2 for concrete) and if the density of the concrete or asphalt is known then the modulus of elasticity (Young's modulus) may also be calculated.

Detection of the ultrasonic waves in the material is achieved using a Michelson type laser interferometer[3] (Figure 4), which is based on a He-Ne laser having a wavelength of 633 nanometers. Most of the laser light is focused on the specimen surface. A fraction is split off and recombined with the reflected light, and the intensity of the resulting interference is detected at the photodiodes. Any displacement of the surface changes the path length of the probe beam causing a time dependent change in phase of the interference fringe. The output signal from the interferometer is this phase change and is proportional to the displacement of the surface.

The instrument has a very flat response over a wide bandwidth, 0-20 MHz, so it is necessary to reduce sensitivity

to low frequency, relatively high amplitude, background vibrations. The low frequency vibrations are effectively removed, using a phase-locking feedback loop system which mechanically changes the path length of the reference beam to compensate for them. Low frequency disturbances such as those encountered on a bridge when traffic is passing and engine vibrations would be removed also.

The signal to noise ratio, and hence sensitivity of the instrument is strongly dependent on the amount of light reflected from the specimen surface. For a given surface more light can be received by using a highly focused beam. If the sensitivity is still in need of improvement there are two ways of obtaining more light: using a highly reflective coating on the surface, or using a more powerful interferometer laser. The latter step will only be effective if all aspects of the interferometer design are also considered.

3. Description of equipment and operational details

The experimental layout adopted for the majority of trials is shown in Figure 5. The source of the ultrasound is a pulsed, focused beam from a Q-switched Nd-YAG laser of wavelength 1060 nanometers, producing a 75 mJoule, 20ns pulse, resulting in energy deposition at the specimen surface of approximately 5 Megawatts per mm^2 thereby producing a very sharp impact pulseof broad frequency bandwidth.

This pulse causes ablation at the spot where the beam strikes the surface generating Rayleigh, shear and compression waves. The direct surface wave and reflected compression wave may then be detected on the same surface at a position some distance from the laser generation point.

In addition to the compression, shear and Rayleigh (surface) waves generated by the Nd-YAG laser pulse ablating the surface, there is an acoustic air wave also generated by

the laser pulse. This acoustic air wave is a shock wave caused by the rapid heating of the air and the sudden vaporisation of the sample material at the Nd-YAG laser beam impact point. It can be heard as the sharp 'crack' when the laser beam strikes the surface of the material (see 5b, "Same Surface-Separation and Near Coincident Tests").

A Tandon (IBM compatible) personal computer controls the laser firing system, data processing and display using a menu orientated suite of programs. (see Figure 6)

The signal from the interferometer is amplified and passed via a variable bandwidth filter to a LeCroy waveform digitizer and display unit which is triggered each time the laser is fired. The repetition rate of firing the Nd-YAG laser can be varied between 1 and 10 times per second but this is dependent upon the energy required in the laser pulse - for these trials the repetition rate was selected as 4 pulses per second. For each 'run' performed the Nd-YAG laser is fired typically 100 or 200 times and data recorded each time. The digitizer averages these waveforms and the signal to noise ratio is improved by a factor of $\sqrt{N}$ where N is the number of averages. The processed signal is passed to the computer where it is calibrated to absolute values of displacement. The data are stored as a file on disc and can be output to a printer/plotter.

4. Techniques and Experimental Work

The program of experimental work began with tests using two concrete slabs of thickness 35mm and 65mm, each constructed with 10mm aggregate. Their velocities were measured using a pair of 50 kHz piezoelectric transducers in a transmit/receive arrangement, direct transmission method[4] and yielded the values 3.5mm per microsecond and 3.7mm per microsecond respectively. These concrete slabs were used during the initial experiments with the laser system in the

three arrangements shown in Figure 7.

The first of these arrangements, the 'Direct' technique was used initially to determine whether or not the Nd-YAG laser could produce a laser pulse which would ablate the surface of the concrete block and thereby generate enough ultrasonic energy to pass through 35mm of concrete and displace the back surface sufficiently to register a signal from the interferometer. This capability was established for the 35mm slab and the experiment was repeated with the 65mm concrete slab, with similar encouraging results. The 'Direct' technique was also used to check the compression wave velocity values obtained by conventional means. During these tests it became obvious that to appreciably improve the strength of the interferometer signal more He-Ne laser light should be reflected from the surface of the sample, and to this end, the surface of the sample in the beam of the interferometer was coated with 3M 'Scotchlite' glass bead reflective paint. This practice was to be adopted throughout the experimental program for all samples.

Having established that a signal could be generated and detected through these two concrete slabs by the Direct technique (Figure 8), tests were then performed with these slabs using the 'Same Surface-Separation' technique to demonstrate that ultrasonic compression waves could be detected after being reflected from an 'inaccessible' back surface (called 2P-waves), and that surface waves, (R-waves) also generated by the impact pulse, could be detected. A range of laser separation distances was employed in these tests to investigate how the 2P-waves and R-waves behaved with increasing distance between the source laser and detecting laser. (Figure 9). The 'Same Surface Separation' technique was adopted for the majority of the tests hereafter.

Carried out concurrently with the separation tests was the 'Near-coincident' technique which investigated problems

associated with the two laser beams in close proximity, about 5mm. This technique is of interest in thickness measurement and in the sizing of defects - the closer the beams the smaller the geometrical effect and the more accurate the sizing of a defect will be. Problems were encountered with this technique as discussed later in Section 5.

Prior to the commencement of the next phase of experiments the Nd-YAG laser was modified to give a 100 mJoule pulse-increased from the 75 mJoule mentioned in Section 3 of this report. This increase in power gave an improved signal to noise ratio in the interferometer waveforms and also resulted in slightly more material being ablated from the sample surface. However, the surface damage was still negligible - a small pinhole about 0.5mm to 1.00mm deep would be produced by a series of 100 laser pulses.

For the next phase of the work concrete thicker sample blocks of 100 to 200mm were fabricated, again using 10mm aggregate, which contained artefacts and artificial defects in pre-arranged positions. These samples included: an artificial delamination, a large void, a triple void and two reinforcing meshes of different square sizes. The samples were examined by conventional ultrasonic methods to find the compression wave velocities and locate defects. A PROTOVALE CM5 Covermeter was used to locate and check the depths of the mesh in the reinforcing sample blocks. Examining these thick block samples with the laser system (Figure 10) did not pose any major problems. A platform on rollers was set up so that the samples could be horizontally traversed in front of the two beams and different positions on the surface could be examined without having to re-align the sample or re-adjust the laser beams to maintain a constant separation. This system was particularly useful for examining these samples when spatial averaging tests were carried out. These required a series of runs to be performed at different positions within a localised area on the sample surface, without altering the

laser separation.

In the final phase of the experimental program, concrete samples of thicknesses ranging from 100 to 250 mm were made using a larger aggregate (20mm sieve) - this being more representative of aggregate size used in highway construction, and new and aged asphalt samples were also procured. The new asphalt samples consisted of a set of three 100mm thick 'fresh hot-rolled' blocks manufactured to BS 4987[5], each having the same composition in aggregate material - a 10mm size open graded wearing course on top of a 20mm size open graded base course - but differing in relative thickness of wearing course/base course, ie 30mm/70mm, 40mm/60mm and 50mm/50mm. The aged asphalt samples were acquired from a site where the asphalt had previously carried traffic for approximately 10 years until recently, when it was excavated for redevelopment. Two such aged samples were used for laser tests, one having a very prominent delamination in the interface between the top (wearing) course and the bottom (base) course where excavation had caused the two layers to part slightly, and the other, showing no visible delamination in the interface. Some problems were encountered during the scanning of the fresh asphalt samples. The samples distorted slightly while being scanned due to the pliability of the fresh bitumen in the high temperatures of an uncharacteristically hot British Summer. This distortion affected the stability of the phasing of the interferometer beam. Boosted air conditioning alleviated this problem.

The application of liquid to the sample surfaces at the Nd-YAG laser impact point during the pulsing of this laser was also investigated early in the program. The liquid was a light release oil such as 'Ambersil' in aerosol form for convenience of application, but later trials with water instead gave similar results. There were advantages and disadvantages in this technique which are discussed later in the report.

On some occasions a waveform would be obtained which showed multiple peaks which appeared to be regular across the waveform output. This can happen when a body vibrates at its natural frequency and the phenomenon is called 'resonance'. An analysis of the frequency spectrum of such a vibrating body, using a technique called Fourier analysis, would show up this resonance frequency as a large peak among other smaller frequency peaks. A concrete slab can be made to resonate with characteristic frequencies related to its physical dimensions and a technique has been used which determines the thickness of such concrete slabs by relating the resonant frequency to thickness (if the compression wave velocity in the sample is known). On the occasions when 'resonance' appeared in the waveforms, Fourier analysis was performed on the waveform to look for a frequency peak which might relate to the thickness of the concrete sample being used. No such peak was found in any of the waveforms analysed and it was therefore thought that the multiple peaks present in the waveforms may have been due to large pieces of aggregate vibrating within the body of the sample.

Investigation of the effects of electronic filtering of the interferometer signals was also carried out using a variable bandwidth filter. As a result of this investigation, a frequency bandwidth range of approximately 20 kHz up to 1 MHz was used for a large majority of the test runs.

5. Results and Discussion

a) Direct Transmission Tests

The initial tests performed with the 35mm and 65mm concrete slabs were carried out using the 'Direct Transmission' technique to check whether or not ultrasonic waves could be generated by the Nd-YAG laser and received by the He-Ne interferometer and, if so, what information could be obtained from the resultant waveform. Figure 8 shows two

waveforms obtained from the 35mm concrete slab during these initial trials. Although it looks a little small in comparison to the twin peak at ~ 25μsec, the important feature in Figure 8(a) is the arrival of the compression wave (P-wave) which comes in at ~ 10 μsec to be followed closely at ~ 15 μsec by the accompanying shear wave (S-wave). These times relate well to the expected times of 10 μs and 16μ sec as calculated using the compression wave velocity of 3.5 mm/μsec and shear wave velocity of 2.2 mm/μsec for the 35mm block, as established by conventional piezoelectric transducer measurements (see Appendix B, 'Calculations'). The large twin peak at 23 → 25 μsec is possibly due to a piece of aggregate being excited under the interferometer beam. Figure 8(a) seems to confirm this since an interferometer beam movement of 5mm away from its previous position in line with the impact epicentre, shows that these localised vibrations are not so strong, although the P-wave has lost some of its amplitude and now the S-wave has almost been lost in the wake of the P-wave. Also of interest is the presence in both (a) and (b) of the 3P-wave (the second reflection of the compression wave) which appears quite strongly. These waveforms showed that signals could indeed be obtained from concrete using this laser system and that features contained within these waveforms related well to conventional ultrasonic measurements made on this 35mm slab. Similarly, good results were obtained from the Direct Transmission tests with the 65mm concrete slab which had a compression wave velocity of 3.7mm/μsec.

b) Same Surface-Separation and Near-Coincident Tests

Figure 9 shows the results of "Same Surface Separation" tests with the 35mm thick concrete slab. The Nd-Yag and He-Ne lasers were aimed at positions on the same surface of the slab with separations between the laser beams of 10mm, 15mm and 50mm. In fact, these waveforms show the drawbacks associated with the Near-Coincident Technique as attempted in the early stages of the project. As the Near-Coincident arrangement was

a special case of the 'Same Surface-Separation' trials, they were run concurrently. It was found that in the separation tests initially, a large pulse of radiative energy (termed 'Breakthrough') from the Nd-YAG laser was finding its way into the interferometer, producing the enormous peak in the waveforms just after the laser firing pulse. This phenomenon was to haunt the early tests until a slight rearrangement of the optics and better screening of the interferometer relieved the situation at least for separations of 10mm and greater. Another problem with small separations was the appearance of the acoustic wave, which is an airborne disturbance emanating from the sudden heating of the air when ablation of the concrete occurs. It is detected by the interferometer because it is a disturbance of very large amplitude with a fairly high frequency content. This acoustic wave can present a problem if a separation distance between laser beams is chosen such that the acoustic wave arrival coincides with and therefore masks the position of required 'features' in the region of interest in the waveform. For example, if the acoustic wave is detected by the interferometer beam at the same time as the reflected compression wave (2P-wave) off the bottom of the sample, then the latter will be obliterated by the acoustic wave and will not be seen in the waveform output. The acoustic wave which travels at ~ 0.34mm/μsec can be seen appearing at about 42 μsecs in Figure 9(b), whilst the reflected compression wave arrives at about 21 μsecs. The times of arrival of these two peaks in the waveform output depend upon the separation distance between the Nd-YAG and He-Ne laser beams, the compression wave velocity in the concrete and the thickness of the concrete sample. As an approximate guide, if the compression wave velocity in a concrete sample is 3.4mm per microsecond, to ensure that the reflected compression wave arrival comes before the acoustic wave arrival, and is not masked by it on the waveform output, the separation distance between the two laser beams must be greater than one-tenth of the total path length travelled by the compression wave from source to detector (see Appendix B,

'Calculations').

One of the main features of importance in these separation tests was the appearance of the Rayleigh or surface wave (R-wave). This wave has a velocity approximately 0.55 times that of the compression wave velocity in concrete[2]. This value has been substantiated by the results obtained in these tests. The position of the surface-wave arrival obtained from the waveform and the laser separation distance, yield the surface wave velocity which can be used to calculate a value for the compression wave velocity of the concrete. In Figure 9(a) it can be seen that the Rayleigh wave has been lost almost entirely in the 'breakthrough' pulse since the separation of the lasers is insufficient to allow time for the surface wave to appear, whereas, in 9(b) the separation is sufficient and the surface wave is clear of 'breakthrough' at 7.6 μsec. This would give a value of 3.5 → 3.6mm/μsec for the compression wave velocity of this concrete slab which agrees with the value obtained by conventional ultrasonic methods. Figure 9(c) brings to light another problem - if the laser separation is large (~ 50mm) and the surface of the material is rough the surface wave can lose energy making it difficult to find in the waveform. Increased power in the Nd-YAG laser pulse helped to alleviate this problem to some extent.

c) Spatial Averaging

Because of the multiple scattering off aggregate within the concrete producing many 'unwanted' peaks in the waveforms, it was decided to try the technique of spatial averaging. This entailed modifying the Tandon computer program so that multiple 'runs' could be stored and averaged. These runs were carried out using identical laser separation in each case but both beams would be moved simultaneously through a few millimetres to another target area of the concrete for each run. Eventually up to twelve such 'runs' would be added

together and so be spatially averaged. Figure 10(a) is the waveform obtained from the 65mm thick concrete slab for one run of 100 laser pulses. Notice that the R-wave is not very prominent again, being almost lost in 'breakthrough'. Figure 10(b) shows the spatially averaged waveform obtained as a result of averaging twelve component waveforms such as shown in 10(a). The R-wave position has been enhanced, many of the multiple scattering peaks have been moderated but so unfortunately has the 2P-wave arrival which has taken on a ramp-like appearance. This happened occasionally with spatial averaging - some features would be 'brought out', some would be subdued.

For this reason only a few spatially averaged waveforms (such as that shown in Figure 10(b)) were obtained during the experimental work. Other waveforms shown in this report have been digitally averaged but not spatially averaged. Spatial averaging is still considered to be a valid technique, though it may require many tens of digitally averaged 'runs' added together to produce a spatially averaged waveform in which the important features such as the surface wave and 2P-wave arrival peaks are really outstanding against the background level.

Radial averaging has also been considered but was not carried out experimentally because this would have required a more complex optical arrangement than that available. Essentially the technique would involve splitting the Nd-YAG laser beam into several component beams and firing these beams simultaneously at points on the sample surface, equidistant around circumference of a circle with the He-Ne interferometer beam focussed at the centre of this circle. The radial separation between the Nd-YAG laser component beams and the central interferometer beam would need to be greater than the mean aggregate size.

d) Detection of Defects and Artefacts

For the second phase of the work concrete sample blocks were fabricated containing pre-positioned artefacts to simulate a delamination, reinforcing, small multiple voids and a large void. Drawings of these samples and the relevant dimensions appear in the Appendix of this report. Same surface-separation tests were performed on these blocks and the results are now discussed:

i) Artificial Delamination

This sample was constructed with a (100mm x 200mm) sheet of cellophane (~ 1mm thick) sandwiched in the concrete block at a depth of 100mm. Figure 11 is typical of the waveforms received from this sample. The reflected compression wave (2P-wave) back to the top surface of the block is detected nearly 55 µsec after the laser firing pulse. This ties in well with the expected (calculated) arrival time of a compression wave reflected off a delamination at this depth - ie 56 µsec for a total sound path length of nearly 202 mm., using a sound velocity of 3.6 mm/µsec as measured for this block, (see Appendix B, 'Calculations'). Other tests on this block confirmed this feature.

ii) Reinforcing Mesh

Two of these sample blocks were made, one containing a mesh of 2" squares (crossover centres at 2") and the other containing a mesh of 4" squares (crossover centres at 4"). In both blocks the meshes were embedded at a depth of 50mm below the top surface. Figure 12(a) and (b) are waveforms obtained from the 2" mesh samples respectively. There is a definite 'resonance' appearance about the waveform in 12(a) which gave a peak at nearly 500 kHz in the frequency spectrum obtained using the Fast Fourier Transform capability of the LeCroy Waveform Analyser. It is difficult to believe that the mesh could

be sympathetically vibrating at this frequency. Nevertheless, there are features in the waveform between the surface wave arrival and the onset of the acoustic disturbance which look marginally larger or different from the other peaks and these do almost coincide with the calculated positions of the reflected compression wave (2P-wave) at 30.3 µsec, a mode converted PS-wave (or even SP-wave) at 40.0 µsec and a 2S-wave at 49.7 µsec. Initially, this result was treated with scepticism as there were so many peaks in the waveform, but on further analysis there does seem to be evidence of the calculated wave arrivals (2P, PS and 2S) coinciding with peaks that are slightly different in appearance from others in the waveform.

The waveform of the 4" mesh sample block is shown in Figure 12(b). There is a relatively prominent peak at approximately 30 µsec, the position where a reflected compression wave would be expected if the 4" mesh was acting as a reflector. However, it proved difficult to repeat this waveform at other targeted areas on the block's surface, and it is thought that this may have been a 'lucky hit' on the cross wire. Conventional measurements using a 'covermeter' on both these mesh samples gave true readings of the mesh depth with less than 10% error.

iii) Voids

A large void sample block and a triple void sample block were made for these tests to determine if such defects could be seen by the laser system. The small voids in the triple void sample were formed using polythene 'bubble' packing sheet and fixing the hemispherical bubbles back to back with adhesive. Three such bubbles were wired into a shuttering box so they would be held in position, and then covered in concrete. The bubbles, it

was estimated, would have a thickness of approximately 20mm and a diameter of approximately 30mm when compressed in the concrete. For easy reference the three bubbles were designated:

Void 1 - 55mm below top surface of concrete block.

Void 2 - 35mm below top surface of concrete block.

Void 3 - 20mm below top surface of concrete block.

The large void sample was fabricated from a slightly inflated (maximum thickness, 15mm) sealed polythene bag (150mm x 100mm) embedded in the concrete at a depth of 50mm.

Waveforms obtained with the laser beams over each estimated void position on the triple void sample block are shown in Figure 13(a), (b) and (c). The waveforms show that the voids are detectable with voids 2 and 3 giving the strongest signals since they are nearer the surface of the block. In 13(b) and 13(c) there are twin peaks which are quite distinct and even in 13(a) there is the suggestion of a second peak at ~ 38 μsec. It was considered initially that these peaks may be shear waves (2S-waves) reflected off the voids but this is unlikely because they are too close to the 2P wave. It is more likely that these second peaks are due to the compression wave being reflected off the 'flanges' which joined the polythene bubbles together. However, comparison of the 2P-wave peak positions in the waveforms (a) and (c) with the calculated expected positions suggests that voids 1 and 3 are not where they should be. It is possible that they moved when the concrete was poured, in-spite of the wire frame that was intended to hold them in position. The waveforms, however, show very strong signals were obtained from two of these voids. These waveforms were

also repeatable with good agreement and when 'runs' were carried out on this sample block with the lasers well away from the void positions, the waveforms obtained were quite different, possessing no outstanding peaks. Conventional ultrasonic measurements did not give conclusive proof of the depths of the three voids since many differing readings were obtained over the area above these voids.

Figure 14 shows the waveform obtained from the large void sample block. The 2P-wave reflected off the large void has arrived ~ 2 µsec earlier than expected from calculations, indicating that the top of the void is nearer 45mm below the surface of the block instead of 50mm. The 2S-wave reflected off the void arrives at about 46 µsec (calculated at 45.5 µsec) and there is a peak at 58 µsec sitting on a broader base which is the 2P-wave reflected from the bottom of the sample block. Conventional ultrasonic measurements showed there to be an artefact giving a reflection at depths between 40mm and 60mm.

e) Larger Aggregate Samples

For the third and final phase of the experimental work, concrete samples of different thicknesses were constructed using 20mm aggregate sieve. These were to check if signals could be obtained on concrete sections up to 10" thick and also if there was any problem with the 20mm aggregate as opposed to the 10mm aggregate used in the previous concrete samples. There were no known or intended defects in these blocks. Figures 16, 17 and 18 show the waveforms obtained from the 4", 8" and 10" blocks respectively. Some tests were also performed on a 6" block of the same construction - the resulting waveform was similar to that of the 4" block but with a slightly weaker 2P-wave reflected from the bottom of

the block. In Figure 16 the R-wave arrives a little more than 13 µsec after the laser firing pulse. This arrival time fits in well with calculated arrival time of 13.2 µsec for a laser separation of 29mm and compression wave velocity of 4.0mm/µsec. The 2P-wave reflected from the bottom of the 4" concrete block arrives much later (at ~ 58 µsec) than expected (calculated at ~ 51 µsec). There are other peaks of reasonable size in the wake of the R-wave but one in particular at about 38 µsec is probably due to a larger piece of aggregate or a defect. Figure 17 is the waveform from the 8" thick block which had a poor surface finish (powdery in places). Surprisingly, the compression wave velocity as measured conventionally was 4.2 mm/µsec which tends to suggest good quality concrete. The waveform shows the R-wave arriving 2.5 µsec later than calculated (19.5 µsec). This would suggest the surface layer of concrete has a compression wave value of 3.7mm/µsec. The waveform seems to be featureless being flat. The arrival of the 2P-wave from the bottom of the block is barely discernable. This waveform would indicate that the surface quality of this block is deleterious to the generation and the reception of ultrasound by the laser system.

Figure 18 shows the waveform received from the 10" thick concrete block. Although there is more 'character' in this waveform the vital features are not obvious. The R-wave arrives at 27 µsec as a small peak at the tail of what looks like a 'breakthrough' pulse. The calculated value of arrival for the R-wave was 26.5 µsec. The 2P-wave reflected from the bottom of the block is at ~ 136 µsec in agreement with the expected value. There is however, a great deal of resonance in the waveform which has a frequency of about 300 kHz.

f) Fresh Hot-Rolled Asphalt

Three 100mm thick samples of 'fresh hot-rolled asphalt' were produced to BS4987[5], each having a wearing course

composed of 10mm open graded asphalt and a base course composed of 20mm open graded asphalt. These three samples differed only in the ratio of wearing course thickness to base thickness i.e. 30mm/70mm, 40mm/60mm and 50mm/50mm. Figure 20 is the waveform that was received from the 50mm/50mm sample. It confirms to some extent what was expected - that the fresh asphalt would be so pliable that much of the ultrasound energy would be absorbed or damped giving a practically featureless waveform. However, it is interesting that there are slight changes in the character of the waveform where the calculated 2P and 2S waves arrive after reflection from the interface between the 50mm thick wearing course and the 50mm base course, and again at the calculated positions of the 2P and 2S waves reflected from the bottom of the base layer. The arrivals of both the 2S-waves appear to be slightly more prominent than both the 2P-wave arrivals, but this could be too fine an interpretation of this almost featureless waveform. The other two asphalt samples gave very similar results with no obvious definition of the interfaces between the wearing courses and base courses. Conventional ultrasonic measurements did not pick out any reflection of ultrasound from the interfaces in these samples.

g) Aged Asphalt

Two moderately large pieces of 100 → 110mm thick aged asphalt were obtained from a site where the asphalt had previously carried traffic for approximately 10 years until it was recently excavated for redevelopment. The two samples were of identical composition, having ~ 50mm thick, 10mm size close graded (granite) wearing course on top of an approximately 60mm thick, 25mm size close graded (flint) base course. One of these asphalt samples (sample 2) had a very prominent delamination in the interface between the wearing course and base course which covered approximately a third of its area. This was probably due to the excavation process. The other sample (sample 1) had no visible delamination in its

interface.

A typical waveform obtained from sample 1 is shown in Figure 21 with the main features of interest standing out well. The R-wave arrival is at ~ 22µsec (calculated at 22.7 µsec) and the 2P-wave reflected from the interface between the wearing layer and base is probably the first of the two peaks under the 'range bar' on the graph since the calculated position for the 2P-wave from the interface would be at about 37 µsec. The second peak under the range bar could also be a 2P-wave reflection if the wearing layer was 60mm thick. This possible variation of ~ 10mm in the interface position could reasonably be expected. The 2S-wave arrives at ~ 58 µsec (calculated at ~ 60 µsec) with again a possible twin at ~ 70 µsec if a 10mm variation in the interface is accepted. The 2P-wave from the bottom of the asphalt base is calculated to arrive at 73 µsec for 100mm total thickness and from the waveform it can be seen at 73 µsec but, because of the irregularity of the back surface it could have been expected anywhere between 70 µsec and 90 µsec. This waveform shows that aged asphalt can be inspected and thickness and velocity can be calculated provided the surface wave is prominent enough to obtain a value for the compression wave velocity.

The waveforms shown in Figures 22, 23 and 24, are all from the aged asphalt (sample 2) which has the delamination in the interface. The compression wave velocity of this asphalt sample was slightly faster than that of sample 1, being 3.0mm/µsec as measured using conventional ultrasonic transducers. The laser separation distance in Figure 24 is 30mm compared with 40mm separation for Figures 22 and 23. The separation was reduced to boost the R-wave appearance because the rough surface finish of asphalt tends to diminish the amplitude of the surface wave.

Figure 22 shows the waveform obtained from a position on the asphalt sample, well away from the area of the

delamination at the opposite side of the sample. It shows that there is some effect on the ultrasound by the interface.

Possibly the delamination could have extended to this part of the sample, but judgement is reserved on this since sufficient ultrasound energy has crossed the interface to be reflected back as a 2P-wave from the bottom of the asphalt base layer. This accords with the waveform in Figure 21 where there was no visible delamination in the interface of sample 1. The surface wave in Figure 22 has all but disappeared, lost in the surface roughness over 40mm. It should, by calculation be at ~ 23 → 24 μsec and there is a small surface-wave like feature at ~ 22 μsec, but it is not much more significant than the general noise level in the waveform. The 2P and 2S wave reflections from the interface and the 2P reflection from the bottom of the base layer are fairly prominent even though broadbased, arriving within 1 → 2 μsec of their expected times. There can be a wider interpretation of the arrival time of the 2P-wave reflected from the bottom of the base layer as this was very uneven. There are two peaks with arrival times of ~ 15 μsec and ~ 25 μsec which would correspond to 2P and 2S reflections off something near the surface between the lasers. It is more likely that they are due to a compression wave and shear wave being refracted around a surface crack which extends a few millimetres down into the asphalt surface. This would also reduce the surface wave energy or even 'kill' it if orientated at a right angle to the surface wave path to the interferometer. Such cracks were apparent in areas of the surface of the asphalt samples.

The waveform in Figure 23 was obtained from the same asphalt sample as in Figure 22 but the lasers have been moved nearer to the delamination keeping the laser separation at 40mm. The R-wave is a little more noticeable at ~ 23 μsec (calculated at 24 μsec) than in Figure 22. The most obvious feature in the waveform is the 2P wave reflected off the delamination which must extend along the interface of the

asphalt under the laser beam positions. The 2P wave reflected from the delamination arrives at ~ 33.5 µsec, its calculated arrival time assuming a top wearing course thickness of 50mm would be ~ 36 µsec. The 2S wave arrives at ~ 54 µsec whereas its calculated arrival time is 59 µsec. Very little ultrasound energy gets to the bottom of the base layer as can be seen by studying the waveform after ~ 60 µsec. There is a hint of the 2P wave from the bottom of the base course arriving at ~ 64 µsec whereas the calculated time of its arrival is 68 µsec. As all the calculated times of arrival for the R-wave, 2P and 2S waves from the delamination and the 2P wave from the bottom of the base course are consistently later by a few microseconds compared with the actual arrival times in the waveform, it is justifiable to say that the compression wave velocity in this area of the asphalt is slightly faster than the 3.0mm/µsec measured by conventional transducers.

Figure 24 shows the waveform from sample 2 of the aged asphalt with the laser separation now at 30mm (to improve the appearance of the R-wave in the waveform) and the laser beams positioned over the delamination. The waveform shows the R-wave arrival at ~ 15 → 16 µsec (calculated arrival would be 18 µsec). The major feature is the arrival of the 2P wave which has been reflected off the delamination in the interface. It can be seen at ~ 32 µsec in the waveform whereas the calculated time of its arrival is ~ 34 → 35 µsec. The 2S-wave reflected off the delamination shows up at ~ 55 µsec, the calculated time of its arrival is approximately 56 → 57 µsec. Some compression wave energy has managed to get to the bottom of the base layer, to be reflected back and arrive at 66 → 67 µsec which is in keeping with its calculated arrival time of nearly 65.7 µsec.

These results obtained from the tests on the aged asphalt samples are very encouraging since asphalt is considered a difficult material to inspect ultrasonically with conventional

transducers, because of problems with acoustic coupling and contact area. It has to be borne in mind that a thin coating of white reflective paint (glass bead paint) was used throughout all these tests to reflect the He-Ne interferometer beam. Improved sensitivity and a more powerful interferometer laser could render the function of the reflective paint obsolete. It is quite apparent that better results were obtained with the aged asphalt than with fresh rolled asphalt. The bitumen in fresh asphalt has greater pliability and so it more easily absorbs ultrasound energy. It may also prove true that it will be easier to scan close graded asphalt surfaces than open graded since the ultrasound has a better contact path through the material.

h) Liquid Application on Surfaces

During the initial laser trials, experimental 'runs' were performed using liquids sprayed onto the surface of the concrete to study the effect upon the generation and reception of the ultrasound. At first a light oil - 'Ambersil' was used for convenience as it could be applied as an aerosol. Later, water was used, applied to the surface before firing the Nd-YAG laser.

The results of these tests with liquids showed that if the surface was damp or lightly wetted then the generation of ultrasound was not impeded, normally it assisted. However, if there was excess liquid on the surface then the waveform character changed completely, being swamped by resonance type peaks which were generated in the liquid layer. Looking ahead to the situation of scanning a highway surface which is heavily wetted, it may be necessary to provide a blower to remove excess water from the laser target areas. The effect of saturation of the concrete samples with water was not investigated. It is considered that any change in the compression wave velocity, due to water in the pores of the concrete, would be in inverse proportion to the change in the

arrival time of the 2P-wave. This means that depth measurement should be affected very little (see Appendix B, 'Calculations').

i) Reproducibility of Waveforms

The waveforms produced from these laser tests have been reproducible in almost all cases. Where waveforms have shown outstanding features the priority has been to reproduce those findings by repeating the experiment with conditions as near identical as practically possible. The waveform illustrations chosen for the results are a representative selection of the program of work carried out.

6. Conclusions

As proposed, specimens of concrete and asphalt were fabricated which contained simulated defects such as delaminations, voids and reinforcing material for this research program. The ultrasonic responses obtained from these test samples using the laser system have compared favourably with the results obtained by inspection using conventional ultrasonic equipment (50 kHz piezoelectric transducers in transmit/receive arrangement, covermeter and a resonance thickness gauge). The results obtained with the asphalt samples have been encouraging apart from the fresh hot-rolled asphalt samples which were expected to give some problems in inspection. In point of fact, the waveforms obtained from the fresh hot rolled asphalt samples did at least give some information on interface position and overall thickness which was not the case when they were inspected with the 50 kHz conventional ultrasonic transducers.

The laser system, accepting its present limitations, was optimised and developed for the inspection of the concrete and asphalt as the experimental program progressed. The Nd-YAG laser power was increased and the He-Ne interferometer system

optimised. Tests were performed to explore the regimes of waveband filtering and digital and spatial averaging techniques.

The experiments that have been carried out with this laser system and the results obtained, show that there is indeed a positive basis for accepting the principle that lasers can be used remotely both to generate ultrasound in concrete or asphalt, and to detect the responses in these materials to that ultrasound. Specifically, it has been shown from the results of this experimental program that, by using distinct techniques developed for this research program, not only can velocity measurements and thickness measurements be made without resorting to the physical contact of conventional ultrasonic transducers, but that the detection of embedded artefacts and the detection and sizing of defects within concrete or asphalt is also feasible with such a laser based system.

7. Recommendations

In the light of the positive results obtained during the current SHRP-IDEA program it is recommended that further development work be carried out on the laser-ultrasonic system leading to the production of a prototype portable system suitable for field trials.

The development required to reach the prototype stage has been clearly identified during the current programme. The work required may be split into three principle activities involving,

1. Instrument development,

2. Signal processing requirements,

3. Definition of inspection tolerances.

1. Instrument Development

a) Laser Interferometer

The interferometer used for ultrasonic wave detection during this work was a prototype developed at Harwell. As the performance of the interferometer therefore was not optimised for use on concrete, there were some difficulties in operation.

While it was possible to obtain signals from some of the better concrete surfaces, reflective coatings ("glass bead paint") were generally found to be necessary. This made obtaining optical signals easier and increased the signal to noise ratio of the ultrasonic signals (which depends directly on the amount of light reflected from the surface).

Development of an improved interferometer would be necessary to give the sensitivity required with unprepared surfaces. This would involve using a higher power laser in the interferometer than the current 5mW He-Ne laser. Such lasers are readily available and can be incorporated into the current interferometer design.

b) Laser source

The laser and focusing system used could be further optimised to enhance ultrasound generation. Several factors could contribute significantly to this:

i) Pulse length

This influences the bandwidth of the generated ultrasound. As an approximation there is an inverse relation between the pulse length and the peak of the frequency spectrum. As concrete and asphalt are highly attenuating at high frequencies the highest frequency of

interest will be less than 1MHz. This would indicate that an optimum pulse length is about 0.1 → 1 microsecond. There are no readily available laser systems which give beams with this pulse length and optimisation of current systems will be required.

ii) Repetition rate

It is intended that the generation/detection system will scan at reasonably high rates. Also signal averaging may be necessary to improve signal visibility. So the speed of data acquisition depends fundamentally on the repetition rate of the generating pulses. The current laser is capable of pulsing at a maximum rate of 10 Hz. However, current Nd-YAG laser technology allows repetition rates of at least 1 kHz and copper vapour lasers can operate at up to 600 kHz. Increasing the repitition rate is an essential development for the production of a prototype system.

iii) Laser power

The maximum energy available from our laser was 100 milliJoule. Current models routinely supply 1 Joule. Higher energy densities should increase the amplitude of ultrasound generated and hence improve the signal to noise ratio. This may also increase the damage to the surface, but probably within tolerable limits. The amount of the surface ablated depends on the energy density, which depends on the degree of focusing as well as the laser power.

iv) Mobility

As it is required that the instrumentation should be able to scan road surfaces it is essential that it be robust and portable. This criterion is best fulfilled by solid

state lasers such as the one used in this study. A recent development is the use of diode lasers to pump Nd-YAG lasers which offer high repetition rate, high reliability, and very compact laser heads. However more power will be required (about 10 millijoules/pulse) than the 20 microJoule/pulse (approximate) available at present with these pumped systems.

v) Focusing

Conventional circularly symmetric optics were used to focus the beam in this work. However, it may be advantageous to use an annularly focused beam with the interferometer beam at its centre. In this way the signal will be effectively spatially averaged over the area contained by the annular beam. Hence the inhomogenities on the scale of the aggregate size should be averaged out and the signals due to bulk features (back wall echoes, echoes from delaminations) should stand clear. General considerations for focusing are that: the focal length of lens must allow a reasonable stand off distance between the instrumentation and the surface; the depth of focus varies with the focal length and must be sufficient to allow for likely variations in lens-surface distance; the shorter the focal length the sharper the focus. These factors must be optimised when designing a suitable lens system.

vi) Theoretical study

The mechanism of laser generation of ultrasound in concrete has not been extensively theoretically explored. Such a program would be useful in defining the optimisation of the prototype system.

vii) Wavelength of laser light

This should be chosen to optimise absorption. However as absorption is fairly high over a wide bandwidth this is not the most critical parameter.

2. Signal Processing Requirements

The need for effective signal processing to ensure that the significant ultrasonic echoes can be reliably detected and quantified has been demonstrated. Further development of analysis software coupled to the improved instrumentation is required to make maximum use of the data available from the laser ultrasonic inspection system. This work would involve adapting well proven methods such as signal averaging, spatial averaging (or even developing radial averaging as described in section 5c), fast Fourier transforms and frequency averaging for highway inspection.

3. Definition of Inspection Tolerances

In the present work it has been demonstrated that the laser ultrasonic system is capable of measuring features of interest in concrete and asphalt sections. Further work is required to determine the range under which the system can work, the accuracy and repeatability achievable and how these factors relate to the performance of highways. The most useful measurements in the first instance would be the measurement of ultrasonic velocity to relate to the concrete condition and the measurement of thickness. The detection of discrete defects such as voids and delaminations would also be possible.

The use of laser ultrasonic systems could be a major advance in the capabilities of determining the condition of highways in a cost effective manner. The large initial expenditure (in the region of one million dollars) required to develop a prototype laser system as a 'tool' for the

implementation of an integrated highways maintenance program, would be a worthwhile investment in the longer term.

FIGURE 1. LASER PROJECT TEAM : l.to r. Chris Tasker, Fiona Brocklehurst, Ron Smith, Brian Moss.

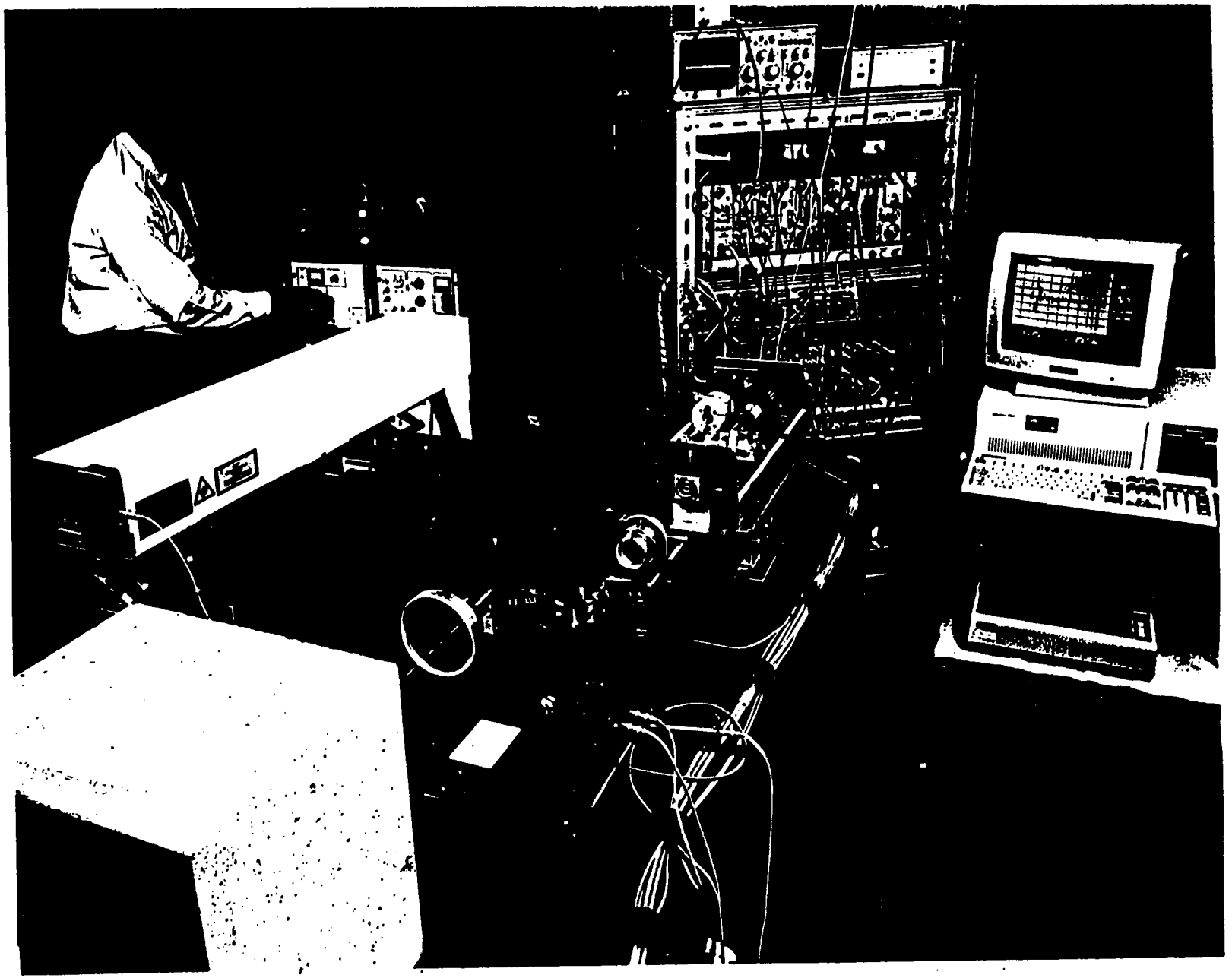

FIGURE 2. GENERAL VIEW OF LASER BASED NON-CONTACTING INSPECTION SYSTEM

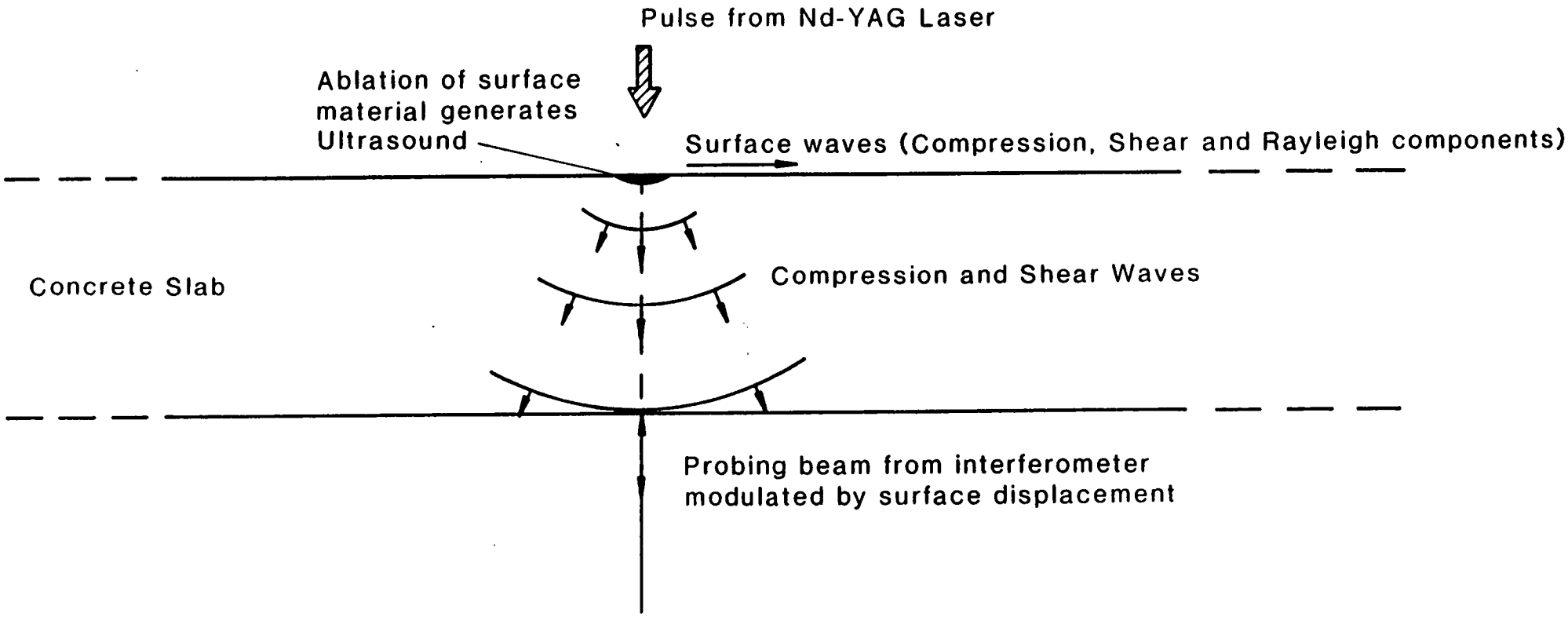

FIGURE 3. PROPAGATION OF ULTRASOUND FROM A HIGH ENERGY LASER SOURCE

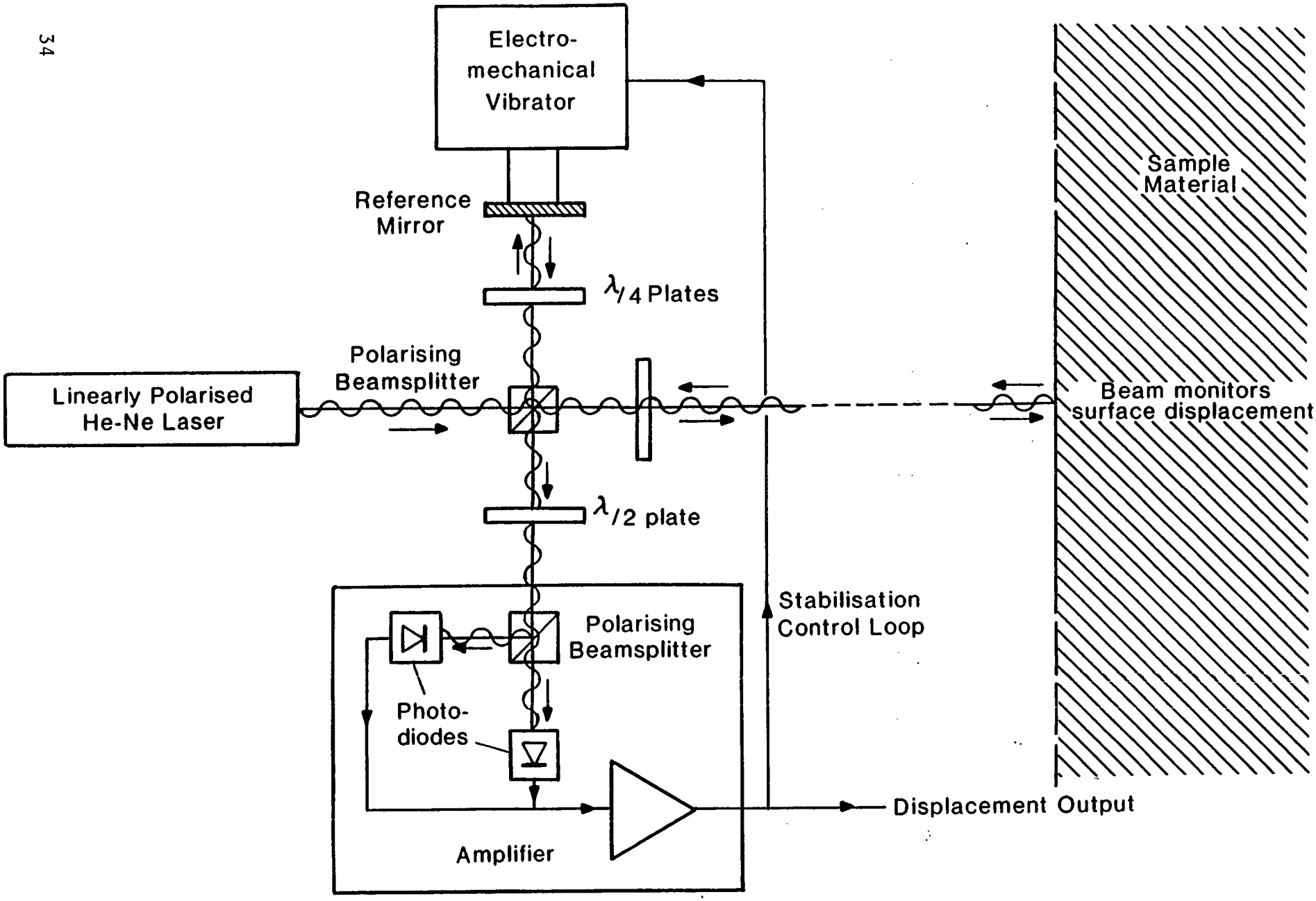

FIGURE 4. He-Ne LASER INTERFEROMETER SYSTEM (BASED ON THE MICHELSON ARRANGEMENT)

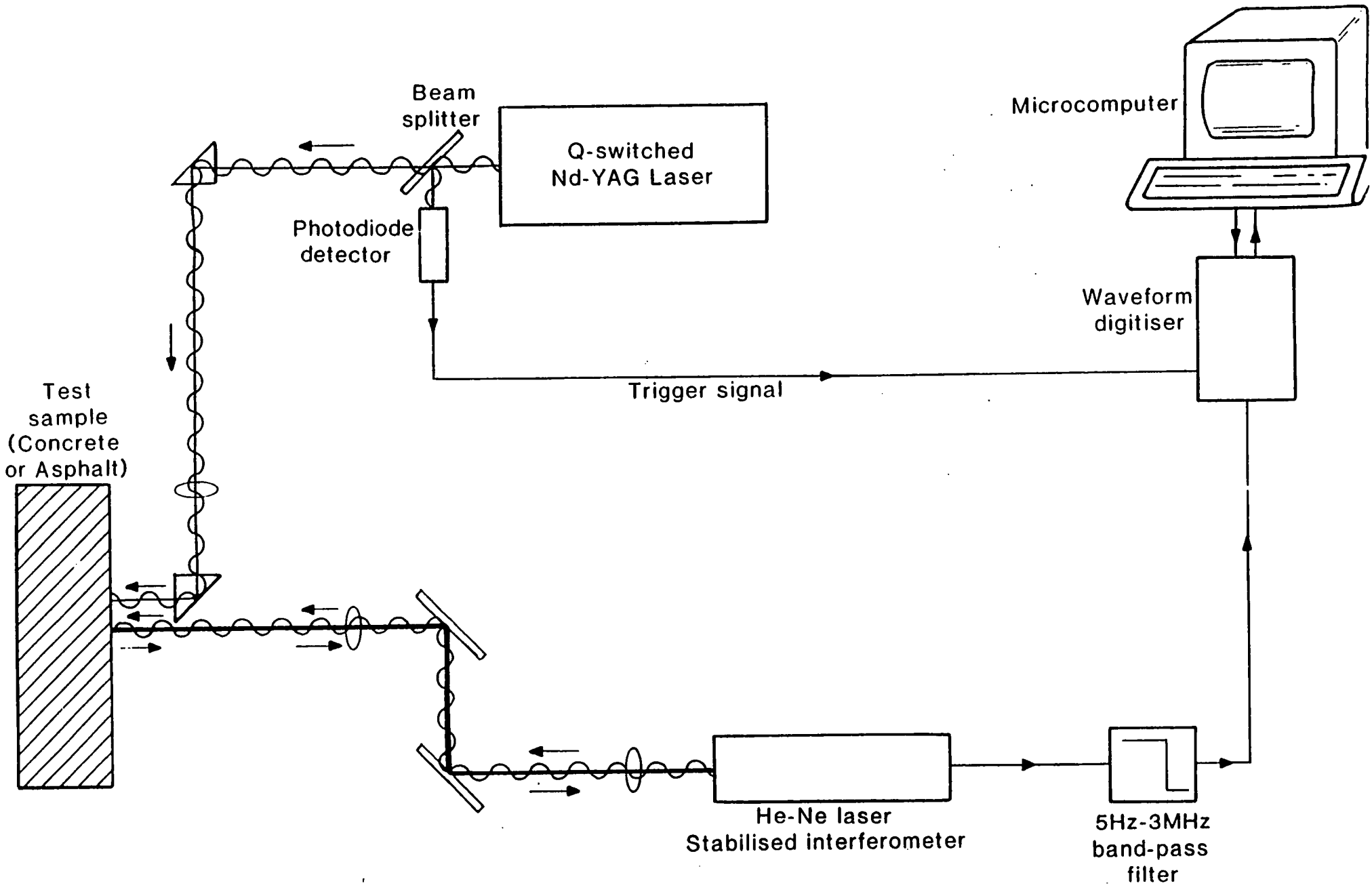

FIGURE 5. SCHEMATIC OF GENERAL LAYOUT OF LASER SYSTEM FOR NON-CONTACT INSPECTION

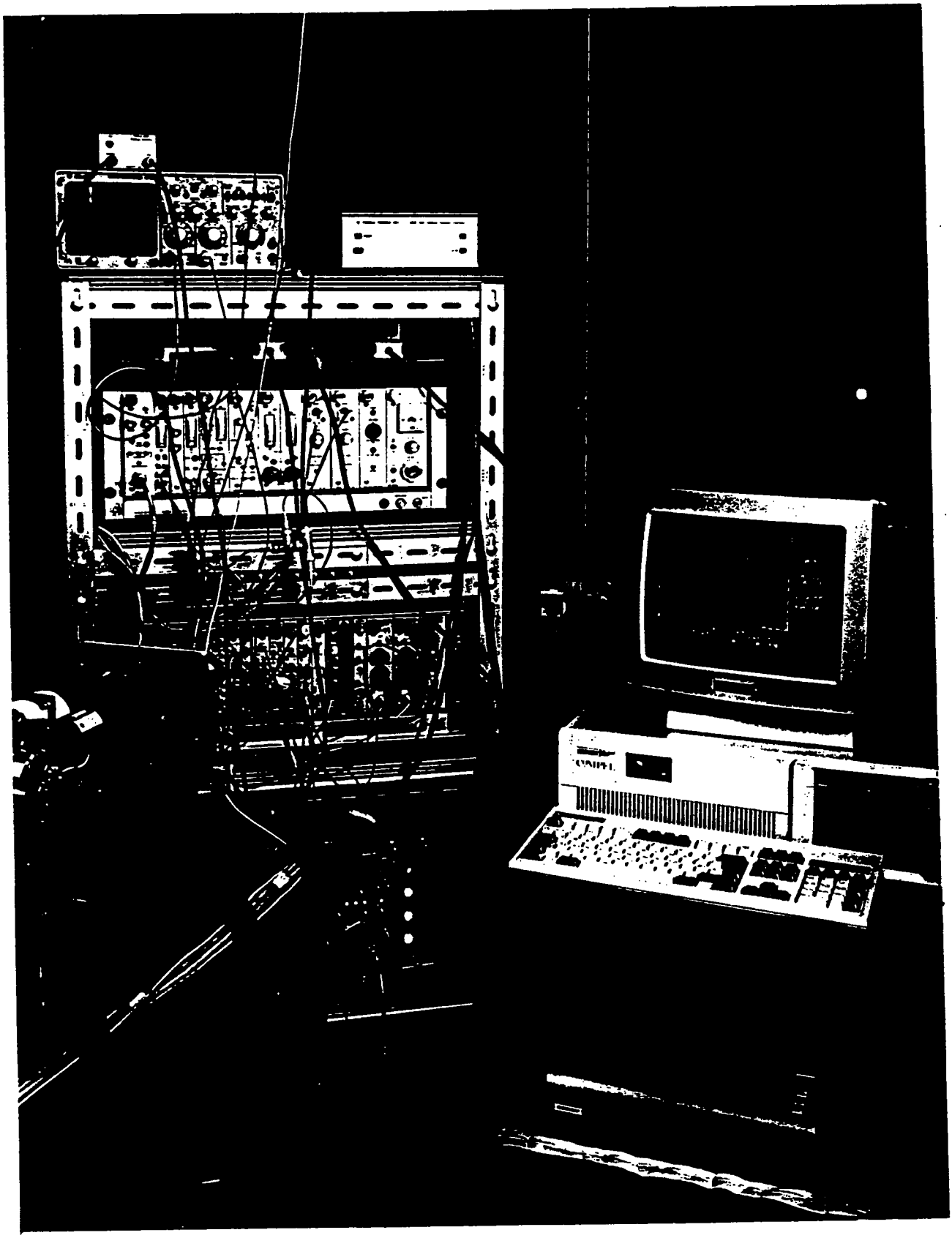

FIGURE 6. LASER SUPPORT ELECTRONICS WITH CONTROL AND DATA ACQUISITION COMPUTER

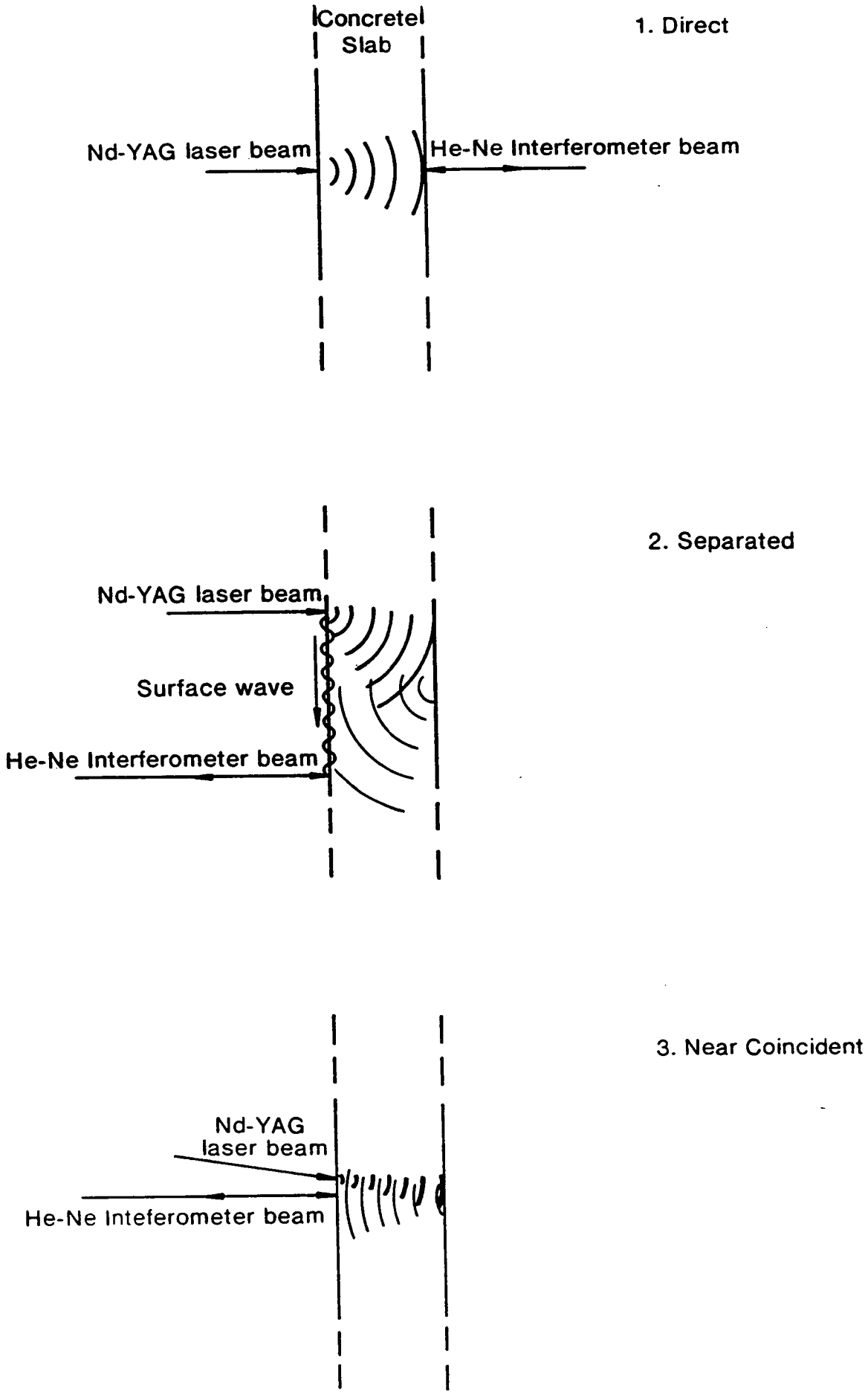

FIG.7. LASER BEAM ARRANGEMENTS AS EMPLOYED IN THE S.H.R.P.-I.D.E.A. TRIALS

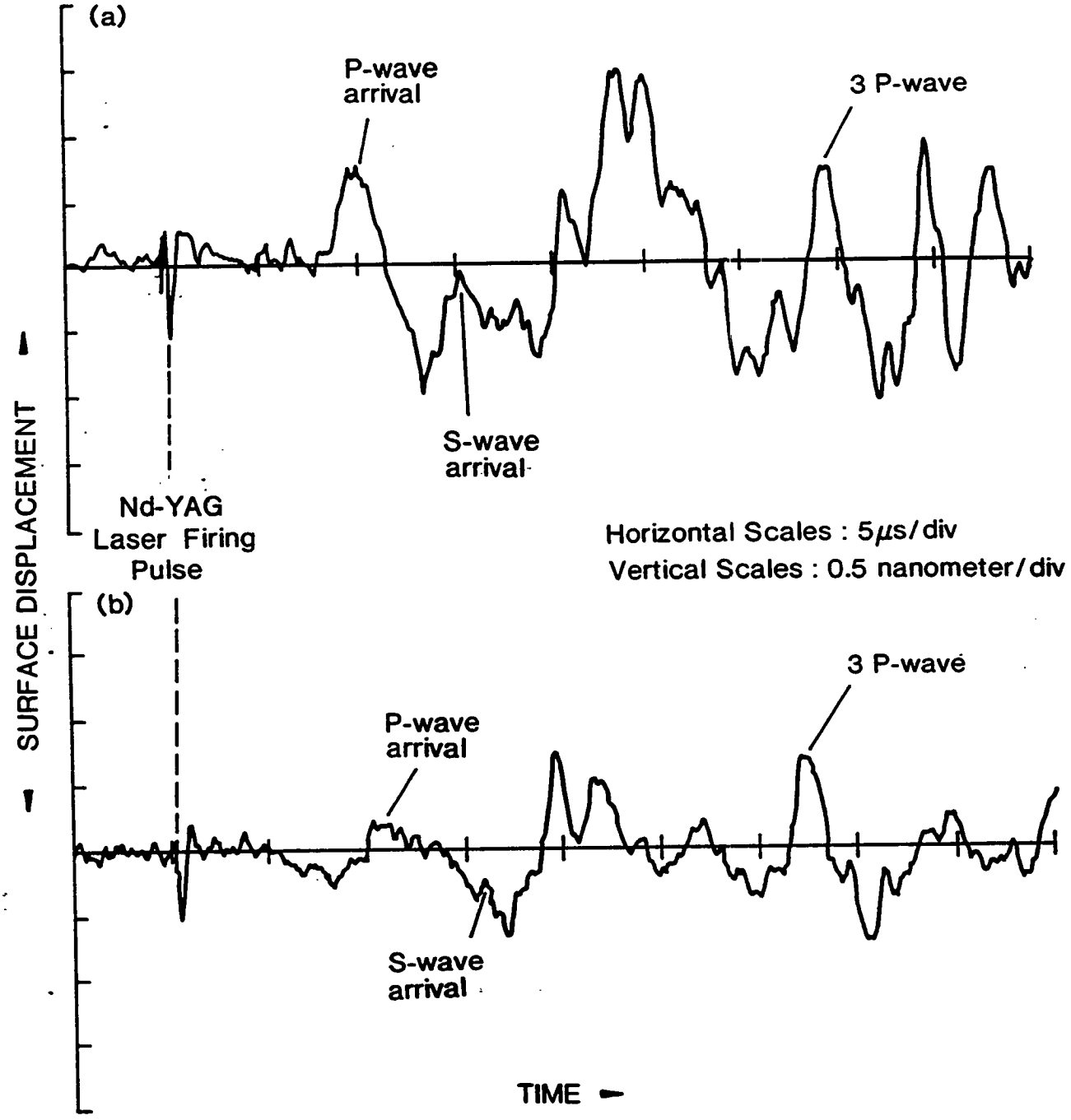

FIGURE 8. INTERFEROMETER OUTPUT WAVEFORMS FROM DIRECT TRANSMISSION TESTS ON 35mm THICK CONCRETE SLAB (a) at impact epicentre (b) 5mm away from impact epicentre. Compression wave velocity for slab ~ 3.5mm/ μ sec.

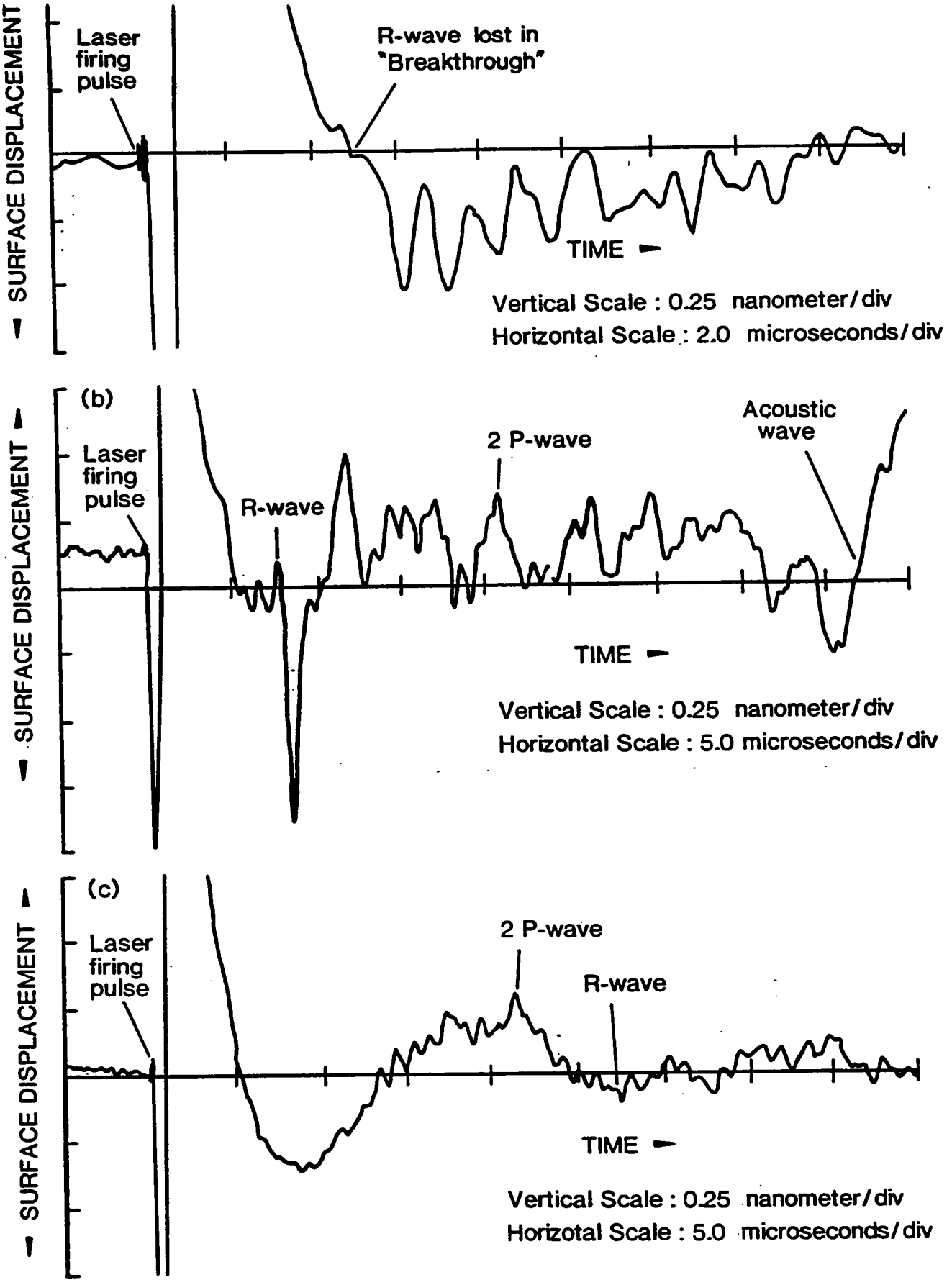

FIGURE 9. "SAME SURFACE - SEPARATION" WAVEFORMS FOR 35mm THICK CONCRETE SLAB. Separation between lasers : (a) 10mm (b) 15mm (c) 50mm. Compression wave velocity of slab : ~3.5mm/μ sec.

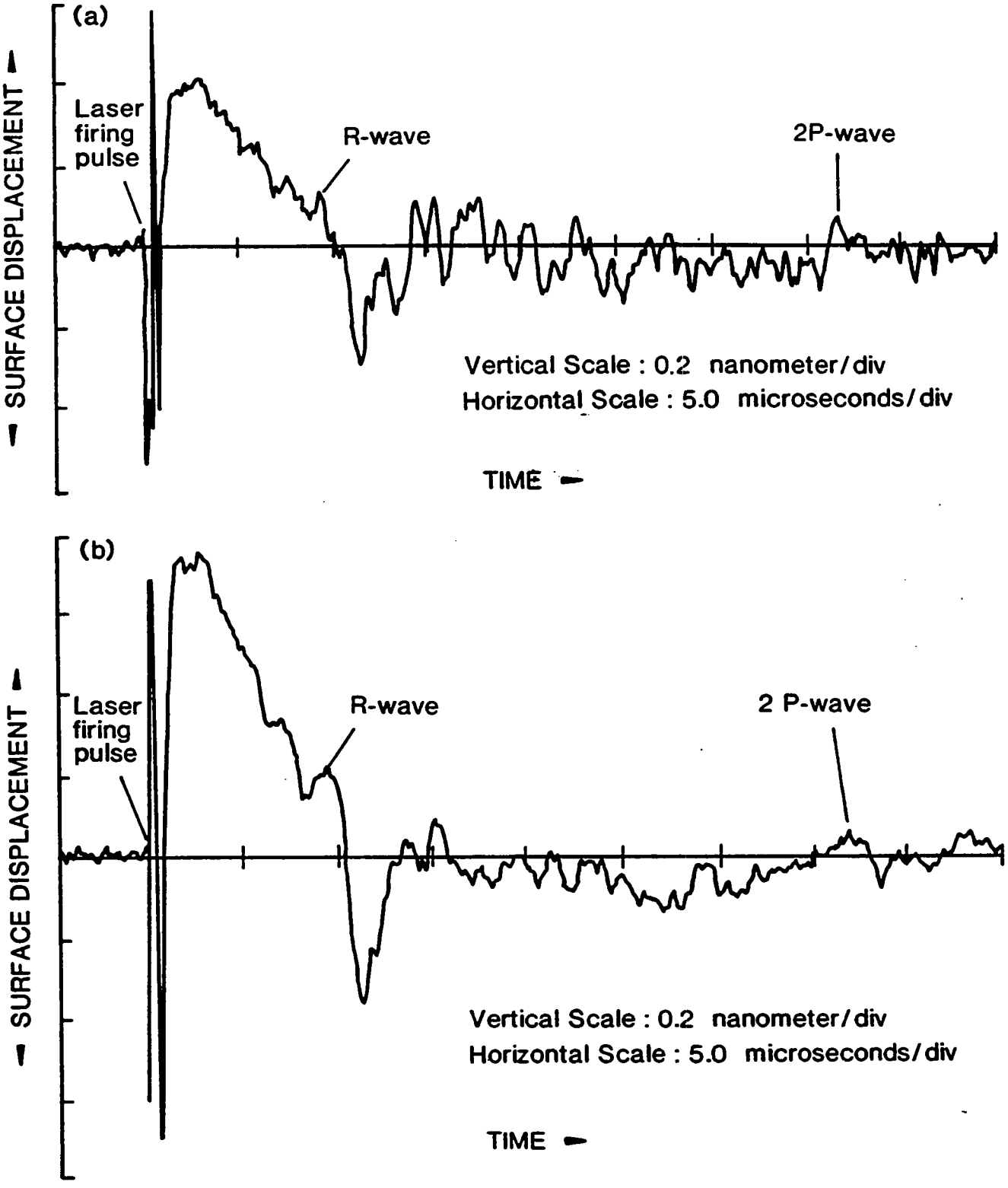

FIGURE 10. SPATIAL AVERAGING : Waveforms obtained using "Same Surface - Separation" technique on 65mm thick concrete slab showing (b) spatially averaged waveform constituted from twelve component waveforms similar to (a). Separation between lasers was 21mm. Compression wave velocity of slab 3.7mm/ μ sec.

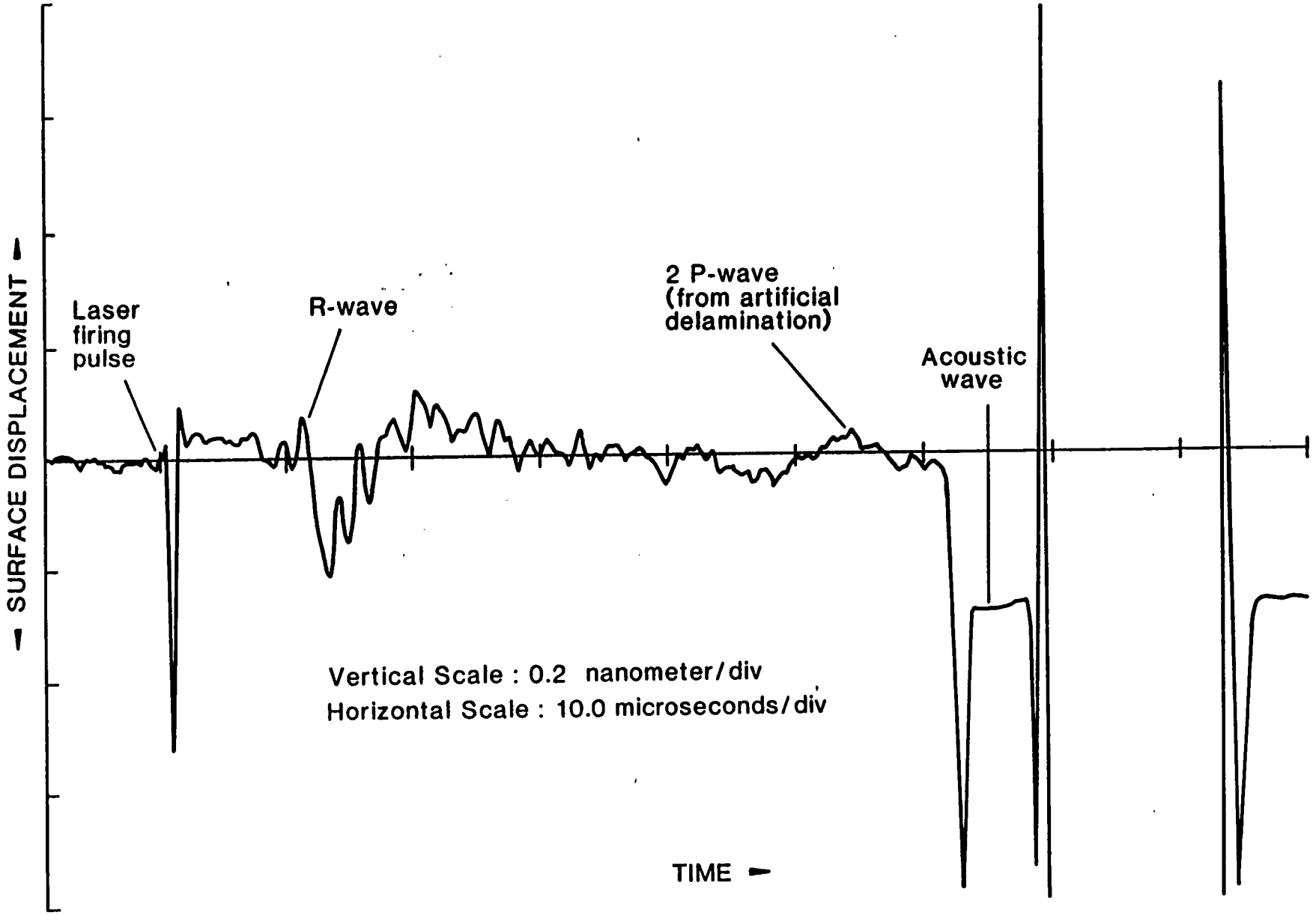

FIGURE 11. WAVEFORM FROM ARTIFICIAL DELAMINATION BLOCK. Delamination size (100mm x 200mm) at a depth of 100mm below top surface of block. Compression wave velocity of concrete : 3.6mm/μ sec. Separation between lasers : 24mm.

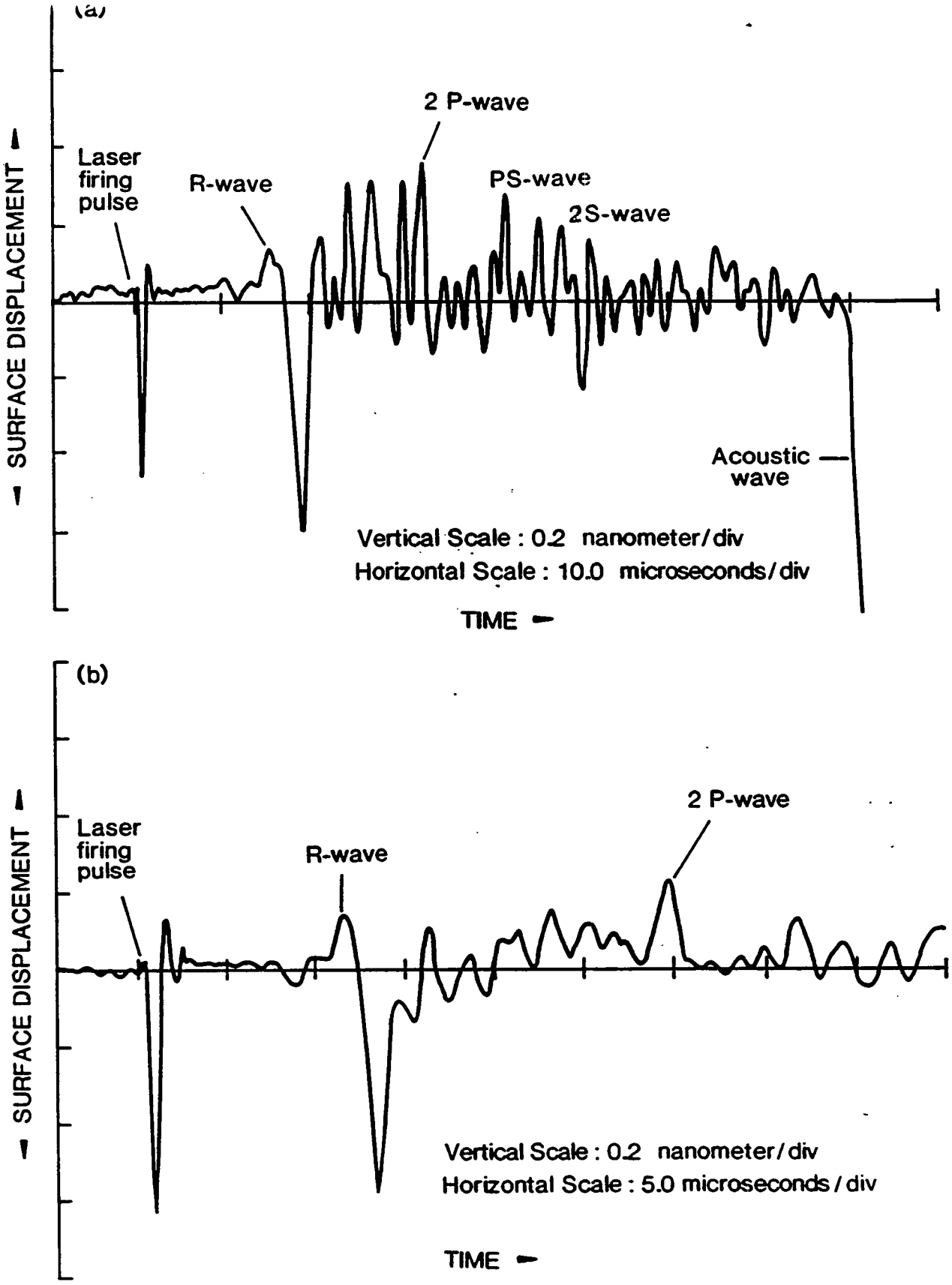

FIGURE 12. WAVEFORMS FROM REINFORCING MESH SAMPLES : (a) 2" square mesh (b) 4" square mesh. Mesh depth was 50mm below concrete block surface in each case. Compression wave velocities: (a) 3.3mm/μsec, (b) 3.4mm/μ sec. Separation between lasers : 30mm.

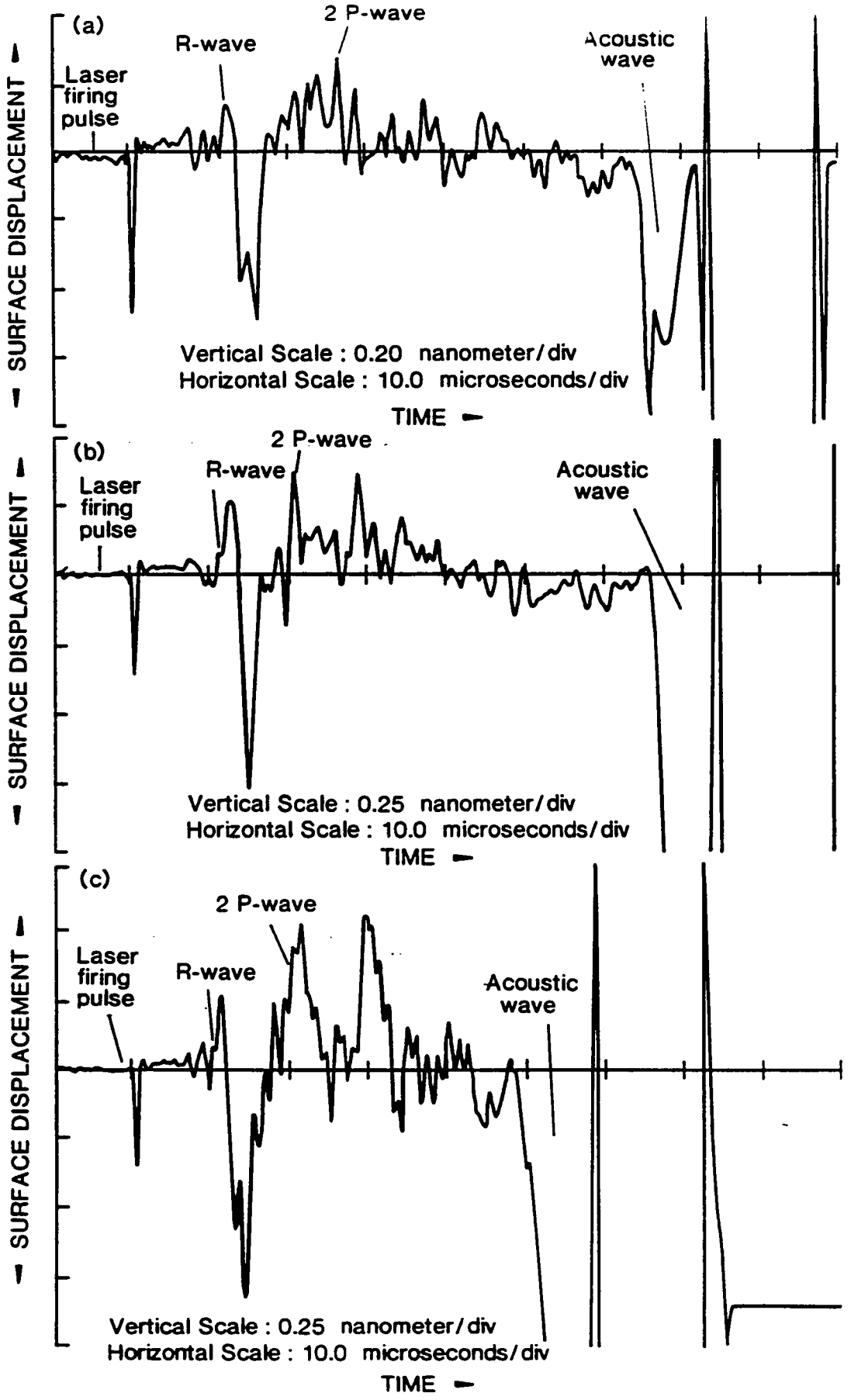

FIGURE 13. WAVEFORMS FROM "TRIPLE VOID" SAMPLE BLOCK : (a) Void 1, 55mm below top surface (b) Void 2, 35mm below top surface (c) Void 3, 20mm below top surface. Compression wave velocity of concrete in sample :3.6mm/μsec Separation of lasers : 26mm in each case.

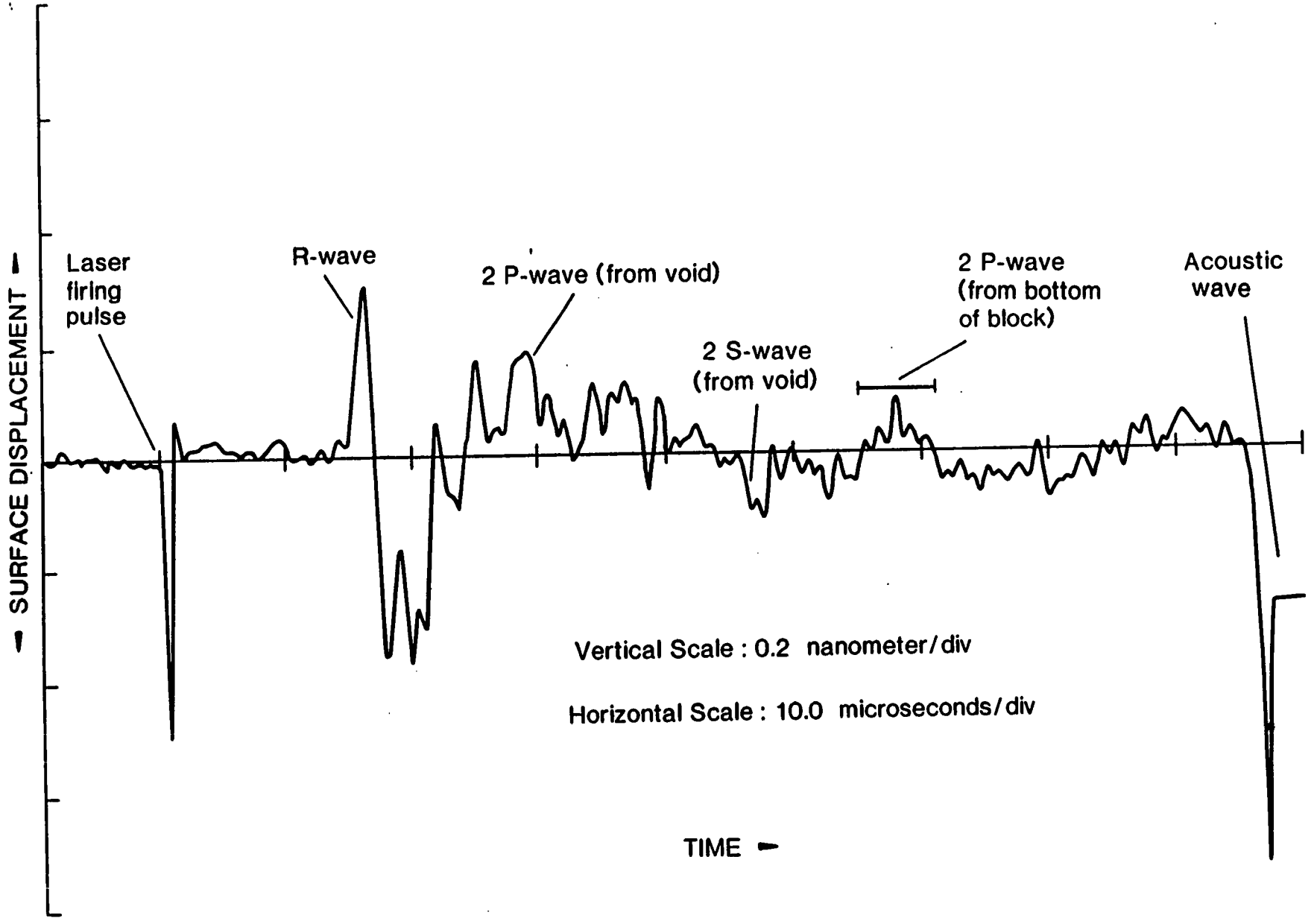

FIGURE 14. WAVEFORM FROM "LARGE VOID" SAMPLE. Void size ~ (150mm x 100mm x 15mm thick) and embedded at depth of 50mm below top surface of block. Compression wave velocity for the concrete : 3.4mm/μsec. Separation between lasers : 34mm.

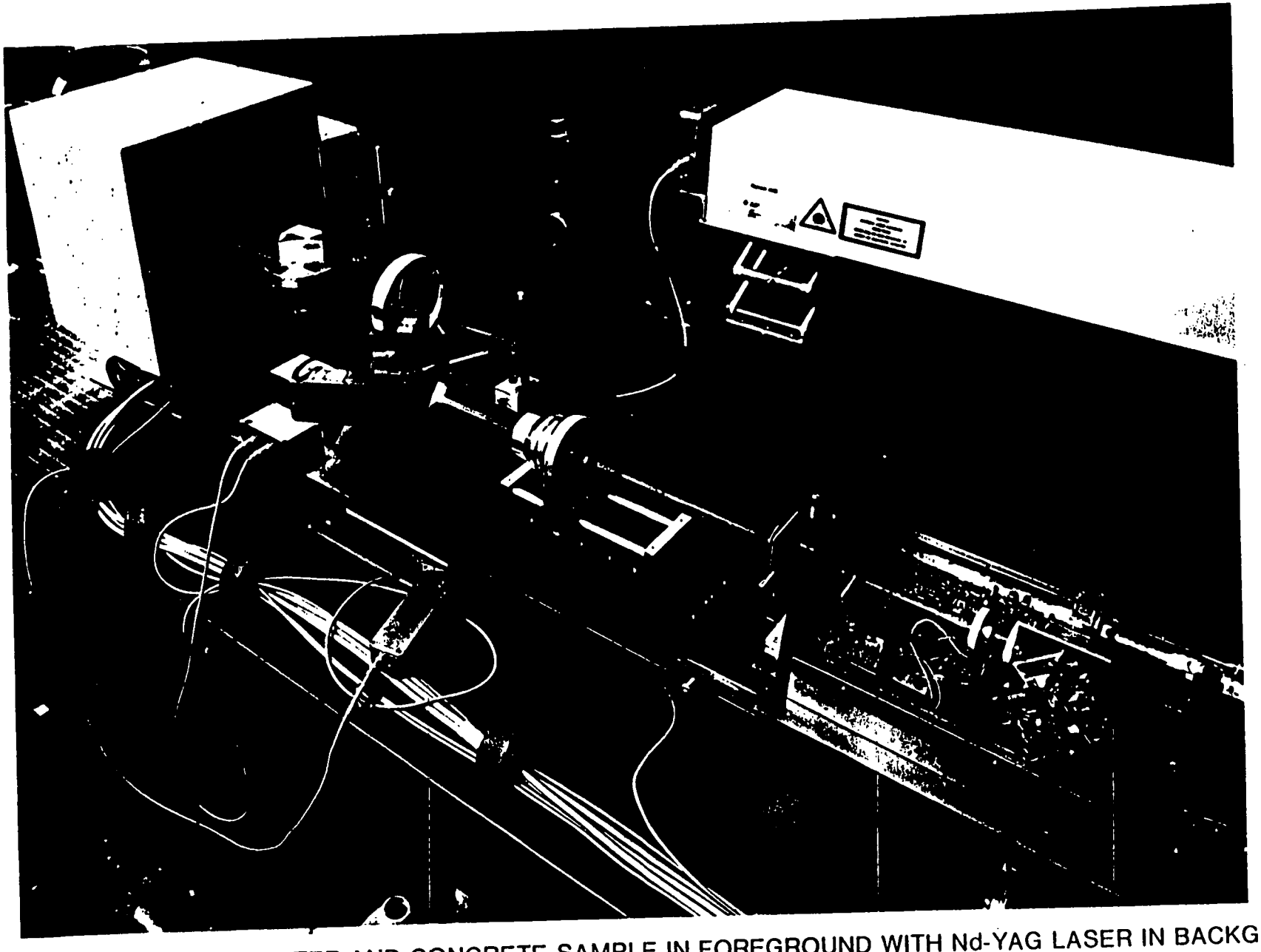

FIGURE 15. He-He INTERFEROMETER AND CONCRETE SAMPLE IN FOREGROUND WITH Nd-YAG LASER IN BACKGROUND

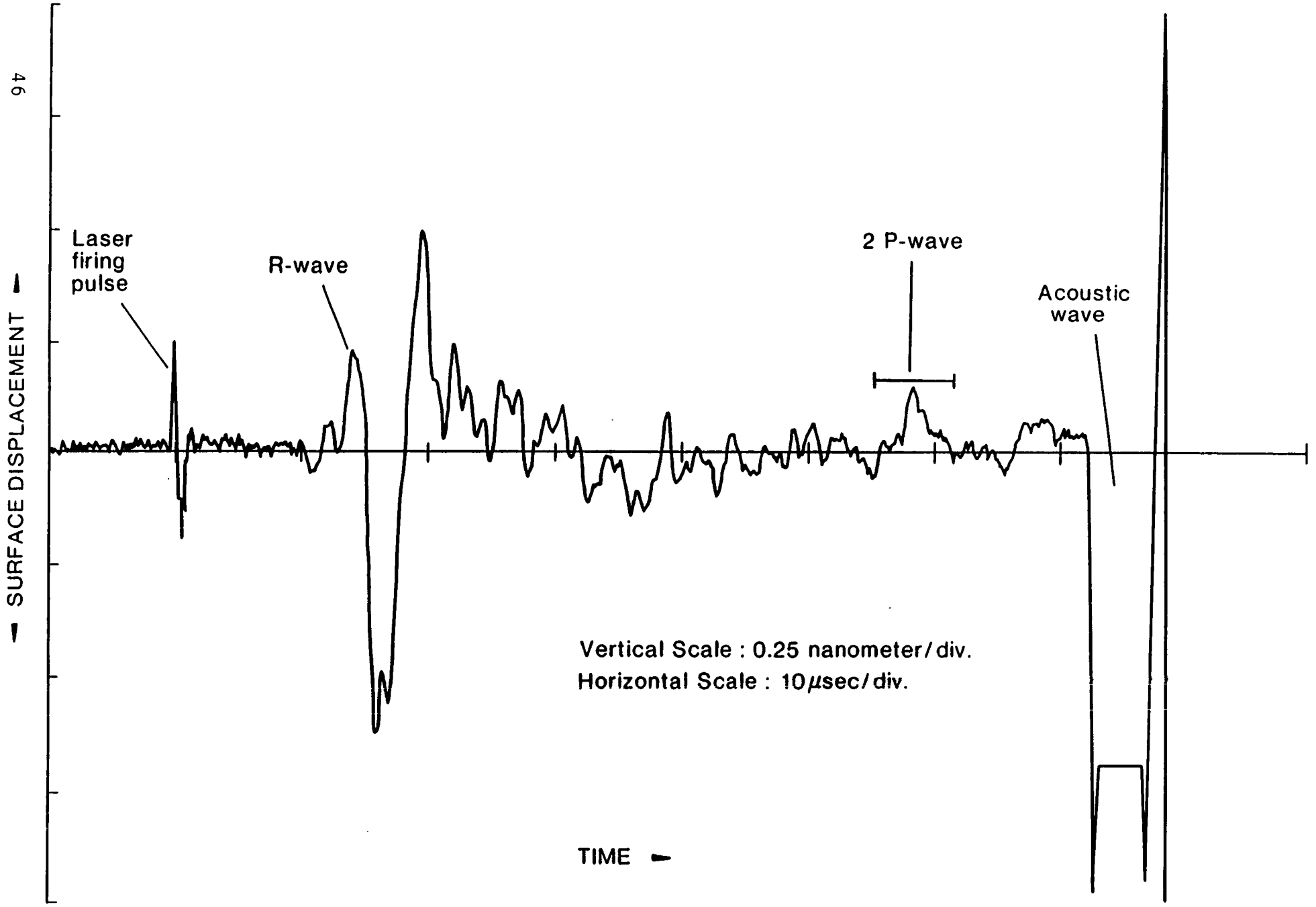

FIGURE 16. WAVEFORM FROM 4″ THICK, 20mm AGGREGATE BLOCK. Compression wave velocity :~4.0mm/μ sec. Separation between lasers : 29mm.

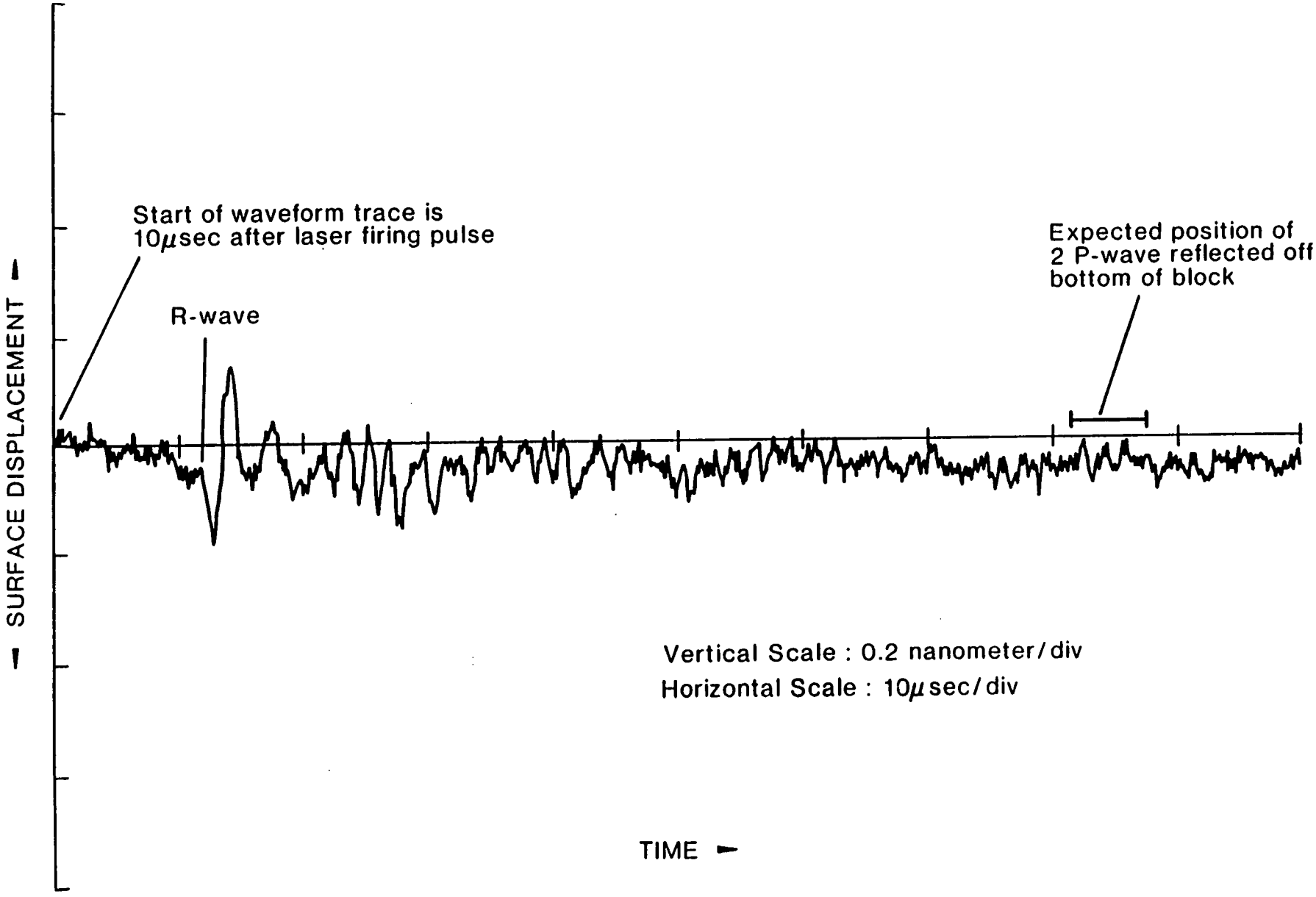

FIGURE 17. WAVEFORM FROM 8" THICK, 20mm AGGREGATE BLOCK (with poor quality surface finish). Compression wave velocity of concrete :~4.2mm/μsec. Separation between lasers : 45mm.

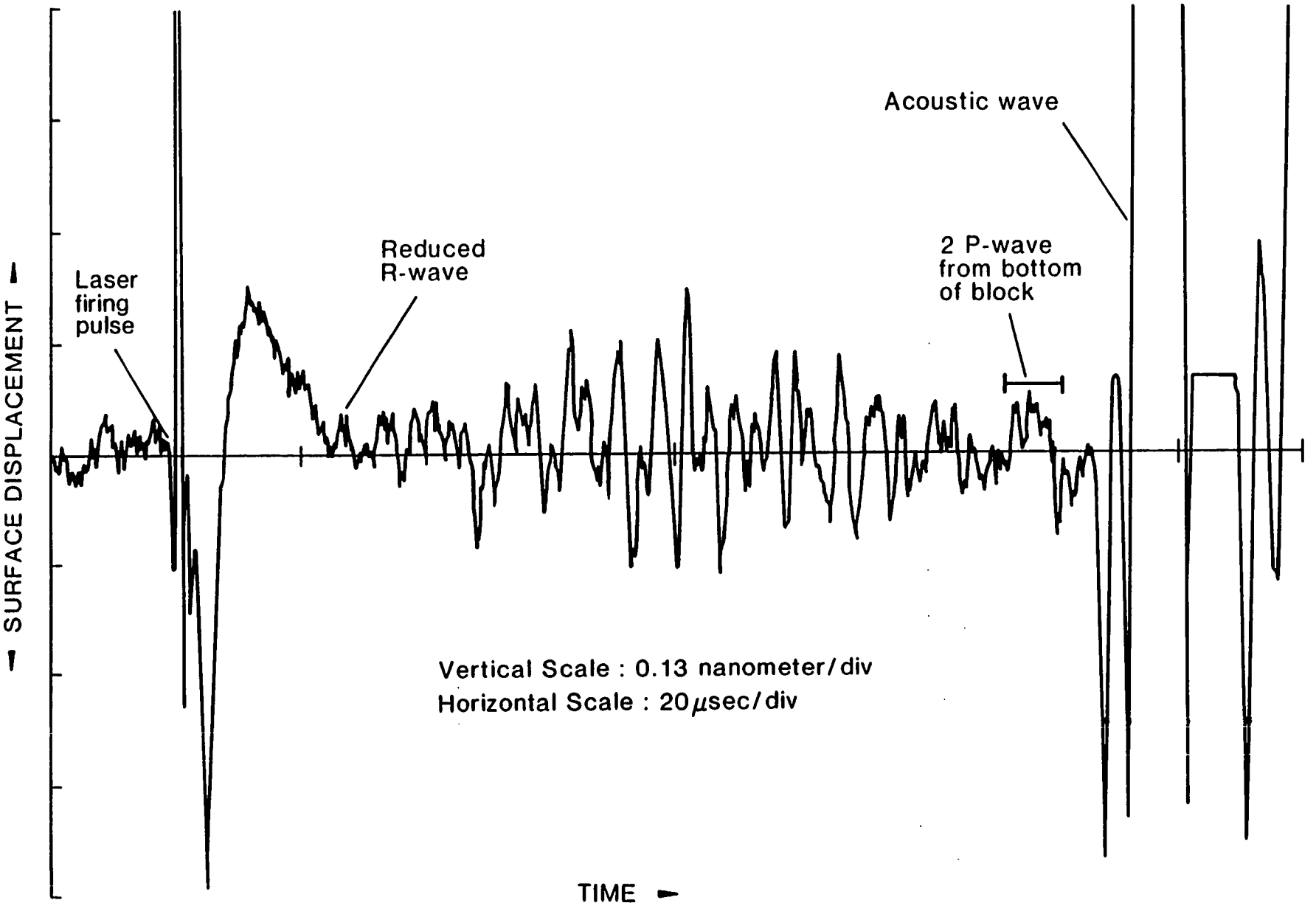

FIGURE 18. WAVEFORM FROM 10" THICK, 20mm AGGREGATE BLOCK. Compression wave velocity :~3.7mm/μsec. Separation between lasers : 54mm.

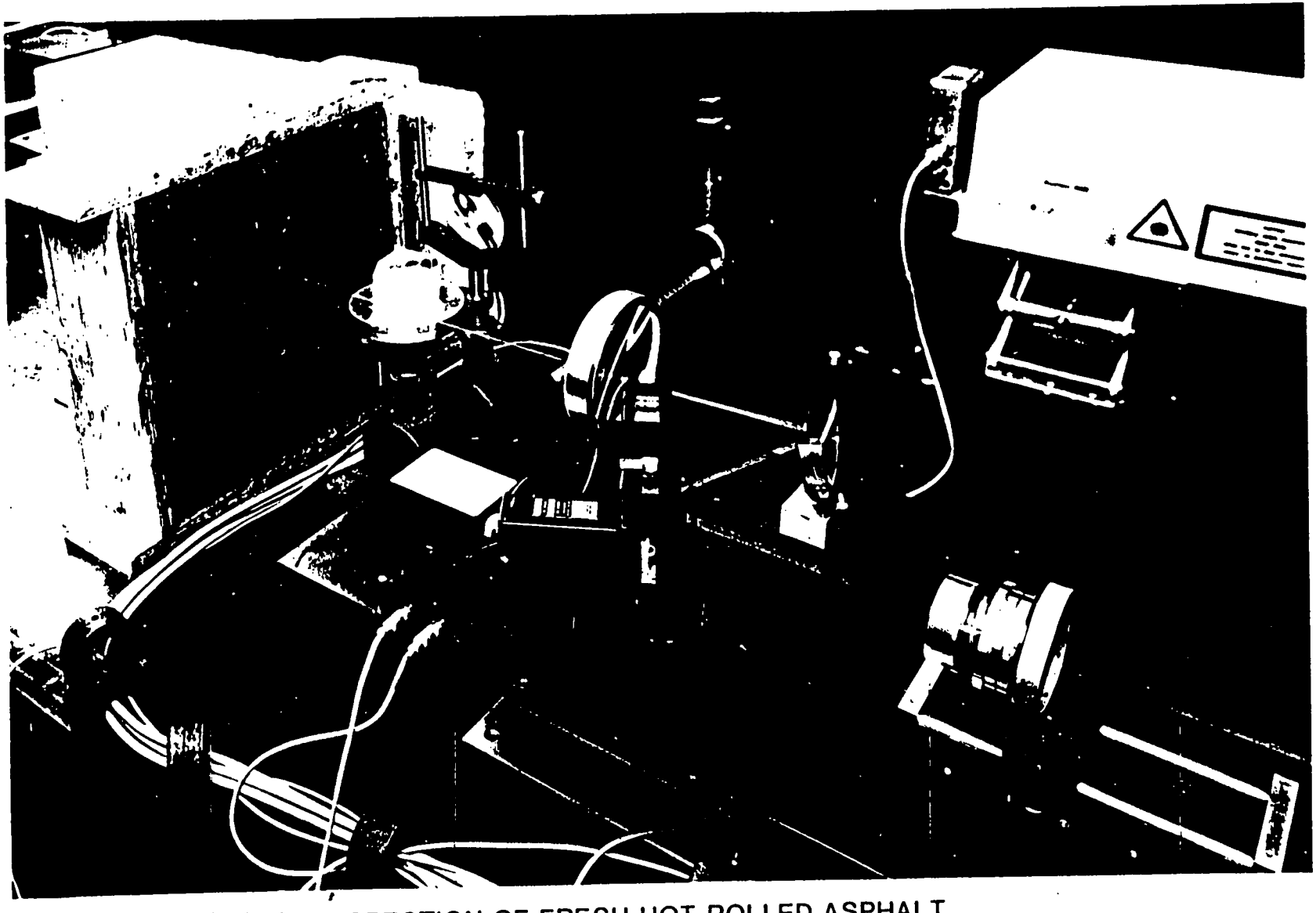

FIGURE 19. INSPECTION OF FRESH HOT-ROLLED ASPHALT

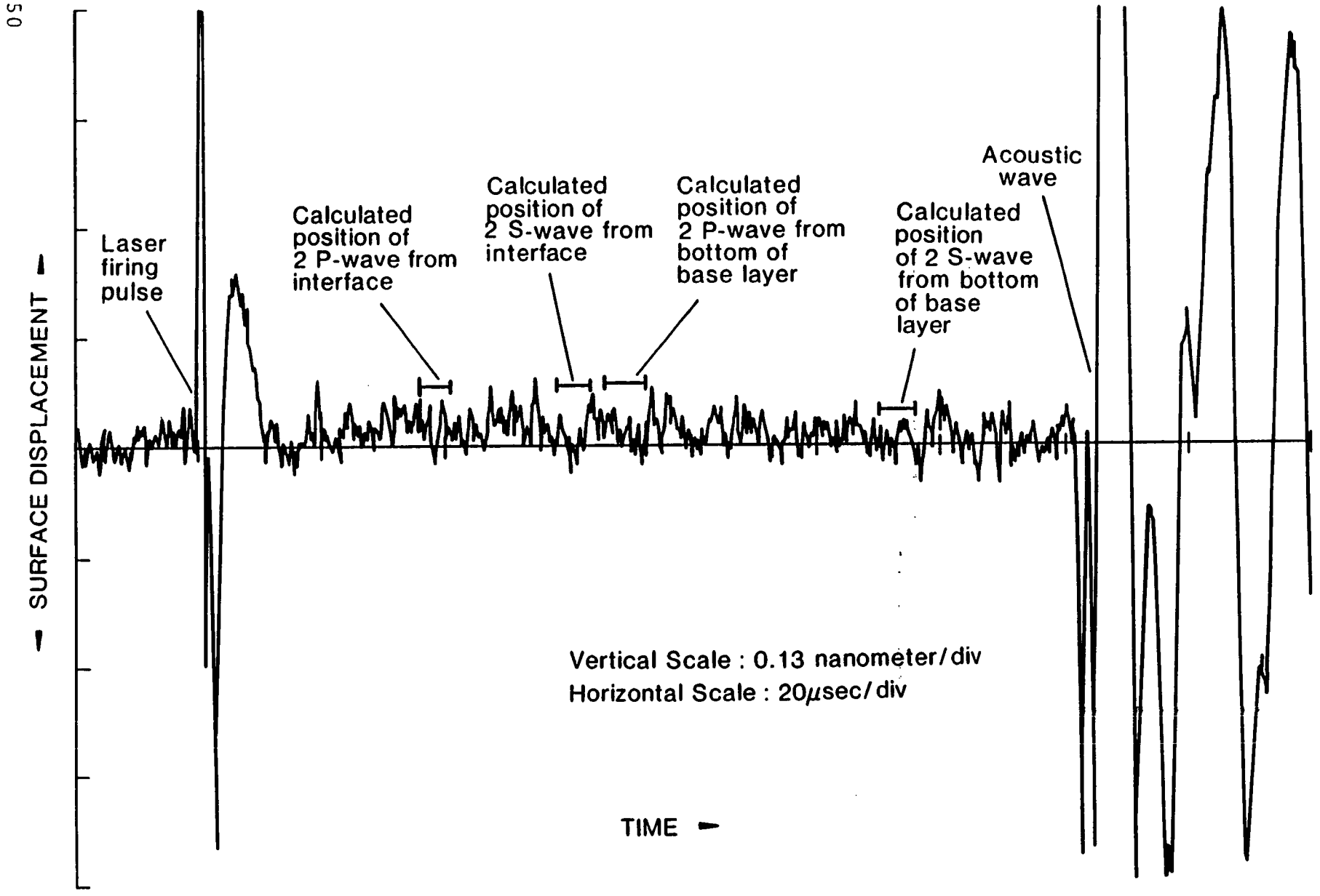

FIGURE 20. WAVEFORM FROM FRESH HOT ROLLED ASPHALT 50/50 SAMPLE. Compression wave velocity : ~3.0mm/μsec. Separation between lasers : 50mm.

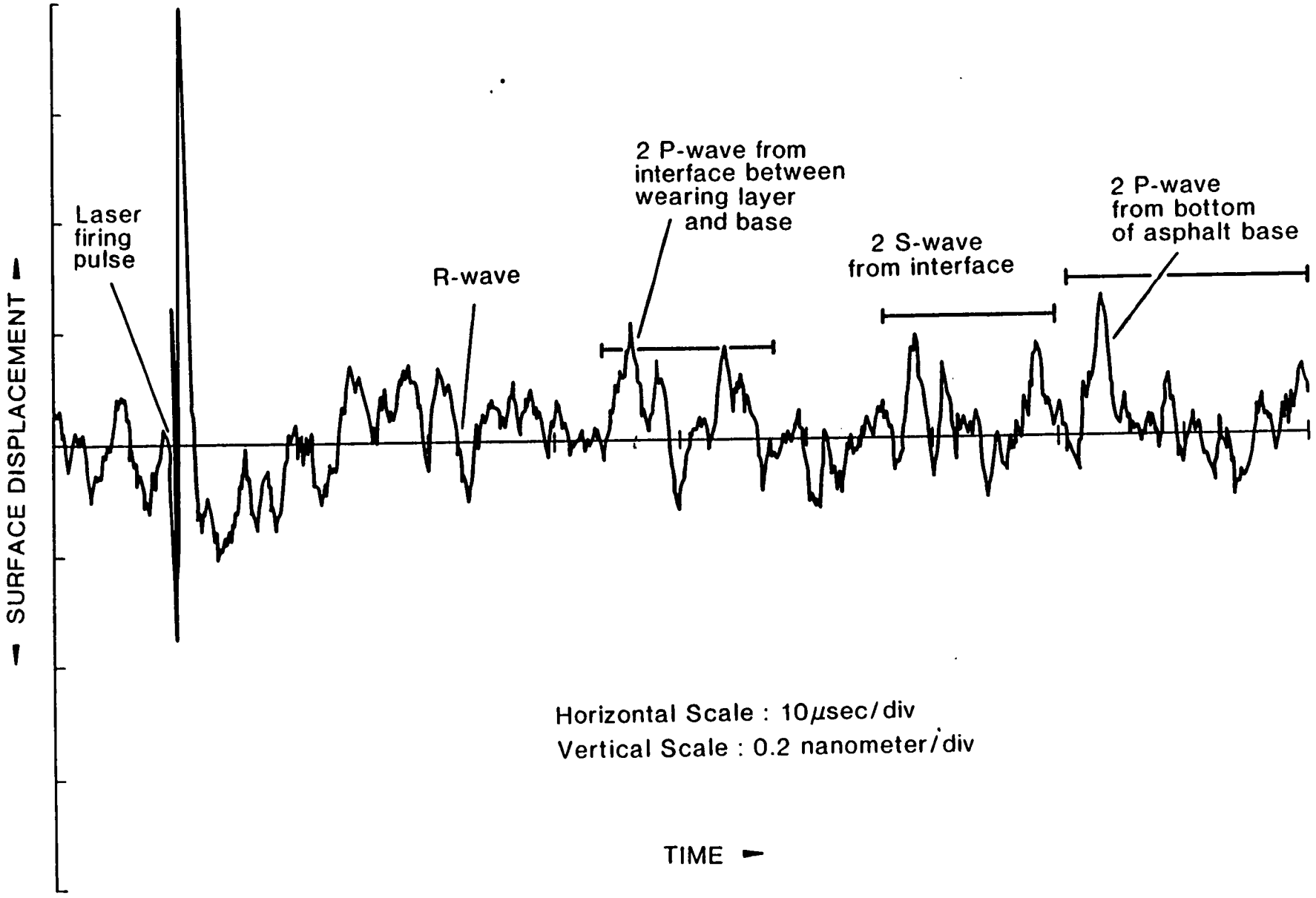

FIGURE 21. WAVEFORM FROM AGED ASPHALT SAMPLE 1. Compression wave velocity :~2.8mm/μsec. Separation between lasers : 35mm.

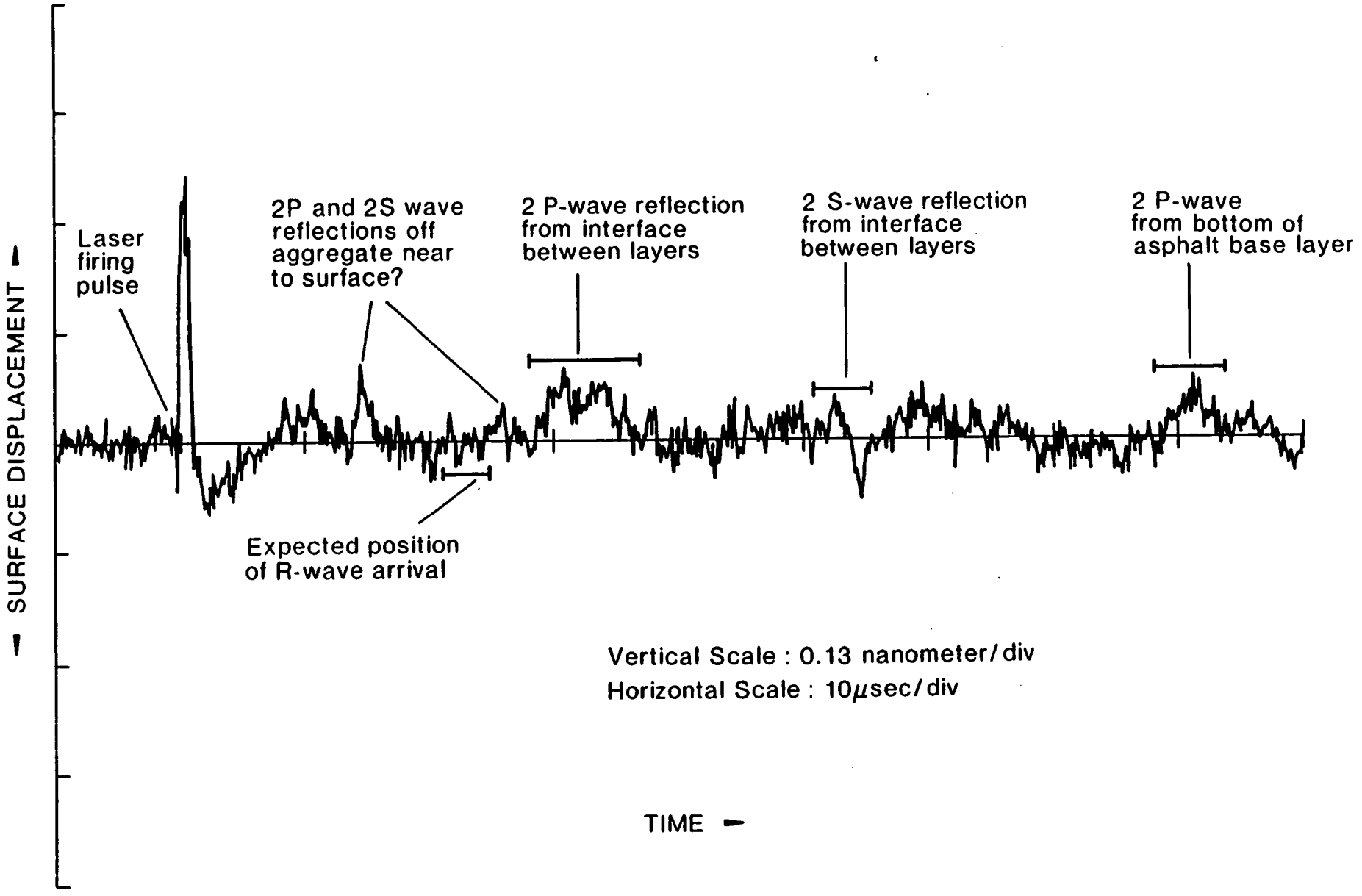

FIGURE 22. WAVEFORM FROM AGED ASPHALT SAMPLE 2. Compression wave velocity : 3.0mm/μsec. Separation between lasers : 40mm. (Position of lasers - away from visible delamination).

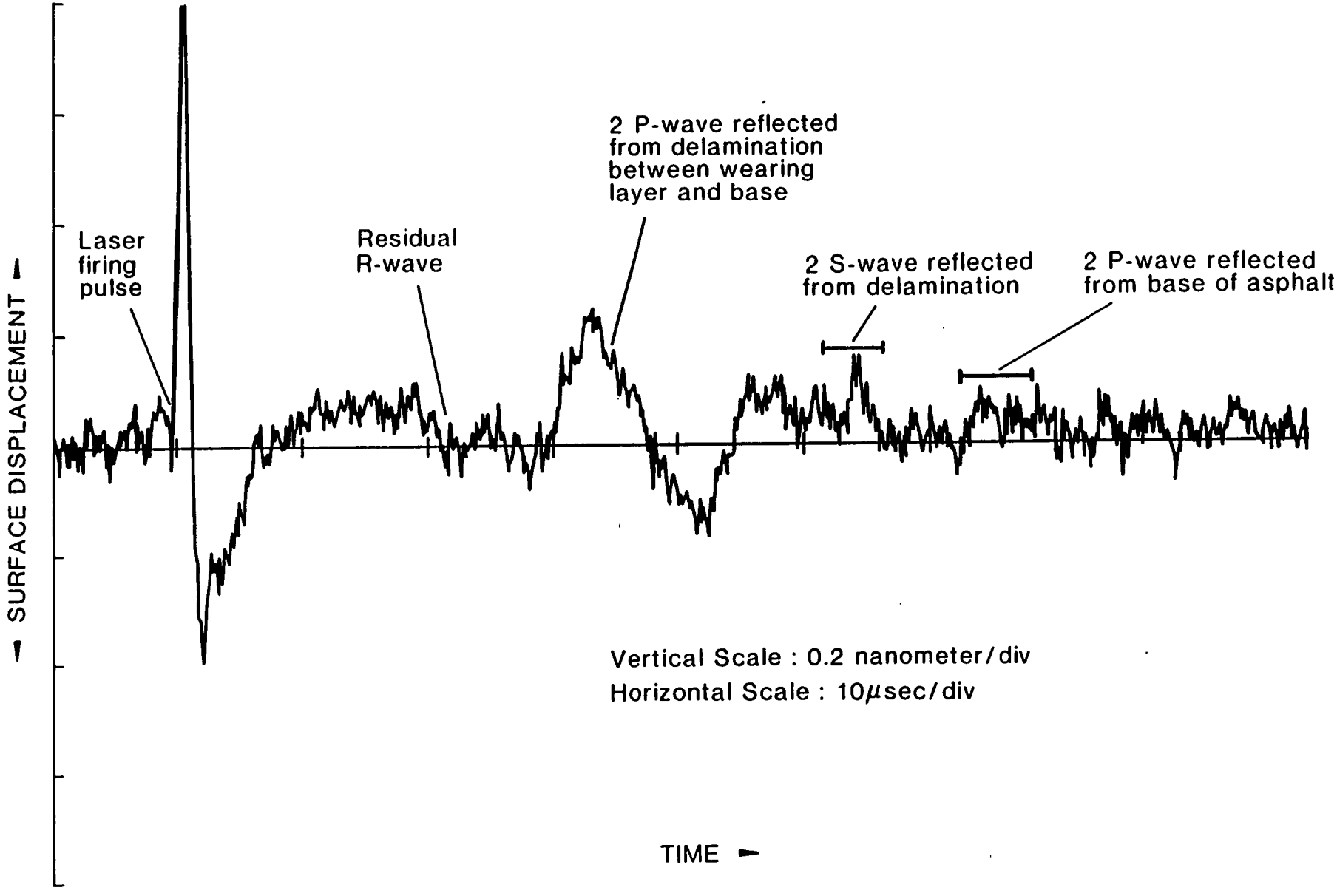

FIGURE 23. WAVEFORM FROM AGED ASPHALT SAMPLE 2. Compression wave velocity :~3.0mm/μsec. Separation between lasers : 40mm.(Position of lasers - near to visible delamination).

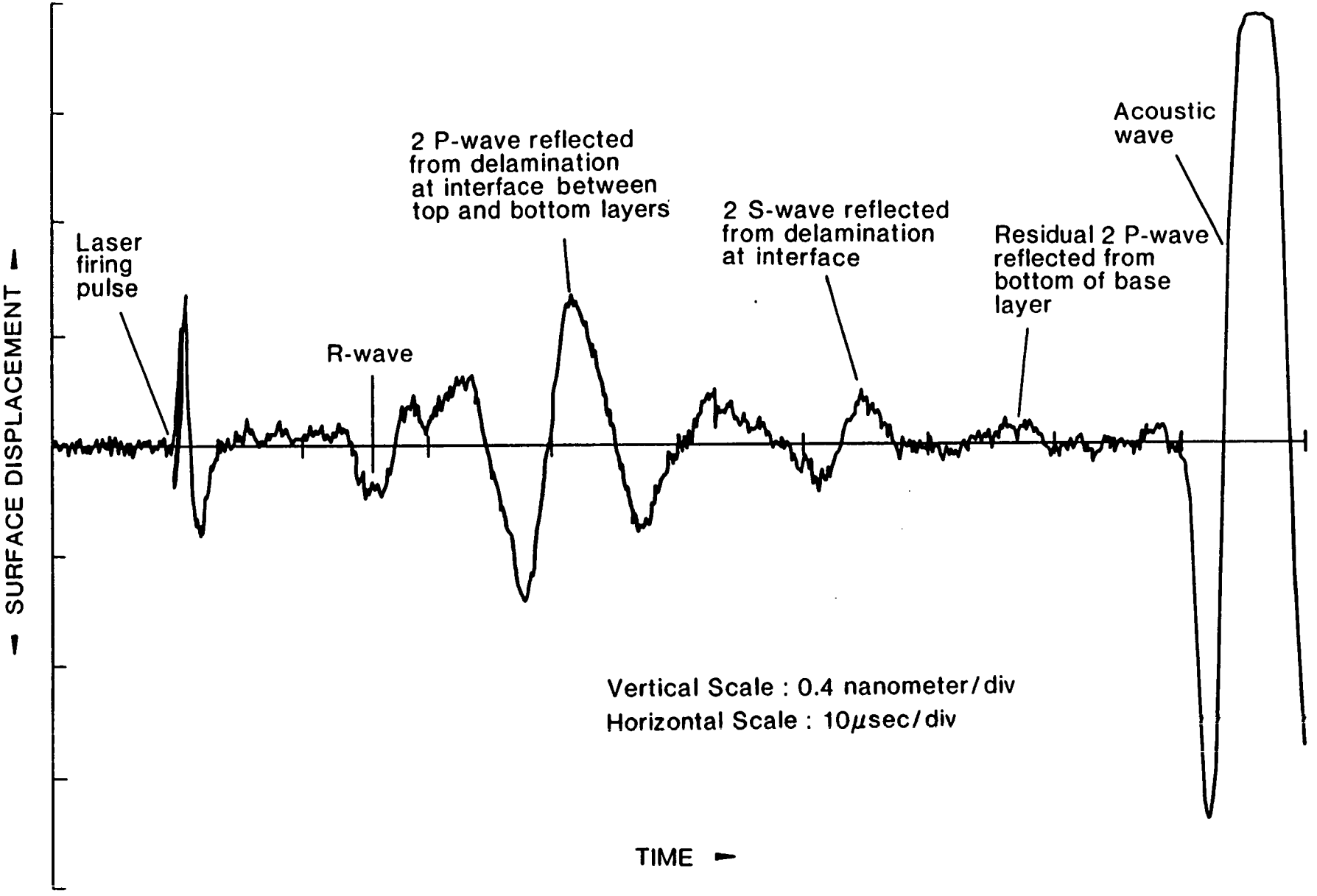

FIGURE 24. WAVEFORM FROM AGED ASPHALT SAMPLE 2. Compression wave velocity : 3.0mm/μsec. Separation between lasers : 30mm. (Position of lasers - above visible delamination).

Table I. Dimensions, composition and compression wave velocities of samples used in tests with Nd-YAG, He-Ne laser inspection system

	Test Sample	Size (mm) (length x width x thickness)	Composition	Compression wave velocity (mm/μsec) (measured with transducers)
1.	35mm slab	450x450x35	10 mm open graded aggregate	3.5
2.	65m slab	450x450x65		3.7
3.	Delamination	300x300x200	100mm sieve aggregate	3.6
4.	Mesh 2"	315x315x150		3.3
5.	Mesh 4"	315x315x150		3.4
6.	Voids (Triple)	300x200x100		3.6
7.	Large Void	300x200x100		3.4
8.	Large Aggregate	280x265x100 (4")	200mm sieve aggregate	4.0
9.	Large Aggregate	300x300x150 (6")		4.1
10.	Large Aggregate	280x265x205 (8")		4.2
11.	Large Aggregate	300x300x250 (10")		3.7
12.	50/50 Fresh Hot rolled asphalt	200x300x100	10 mm open graded asphalt top course (granite)	3.0
13.	40/60 Fresh Hot rolled asphalt	200x300x100	20mm open graded asphalt top course (granite)	2.9
14.	30/70 Fresh Hot rolled asphalt	300x300x100		2.9
15.	Aged Asphalt (1)	540x450x(100->110) Irregular shape	50mm thick top course-10mm close graded asphalt (granite)	2.8
16.	Aged Asphalt (2)	600x600x(100->11-) Irregular shape	50-60mm thick base course-25mm close graded asphalt (flint)	3.0

Appendix A

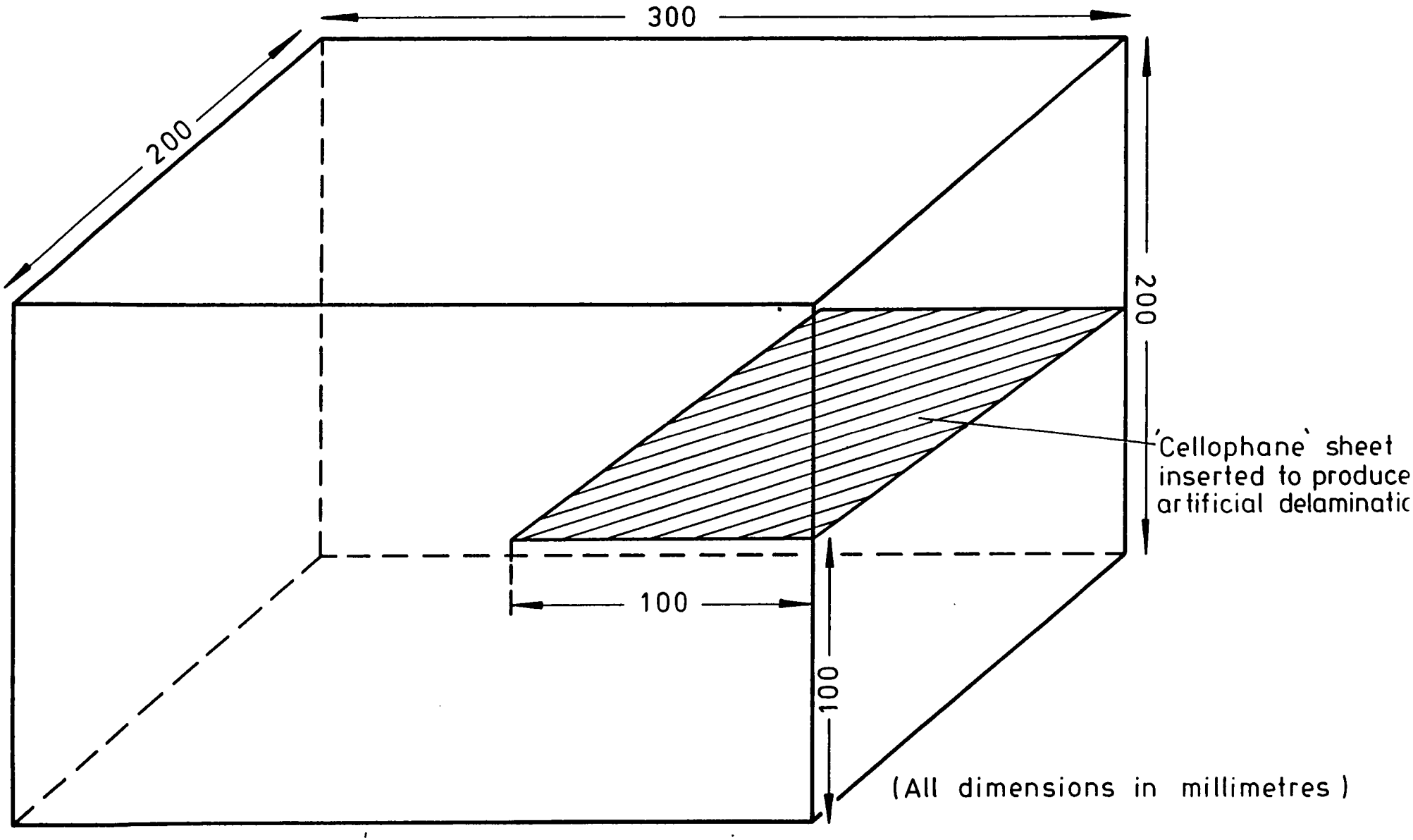

A1 SIMULATED DELAMINATION IN CONCRETE BLOCK.

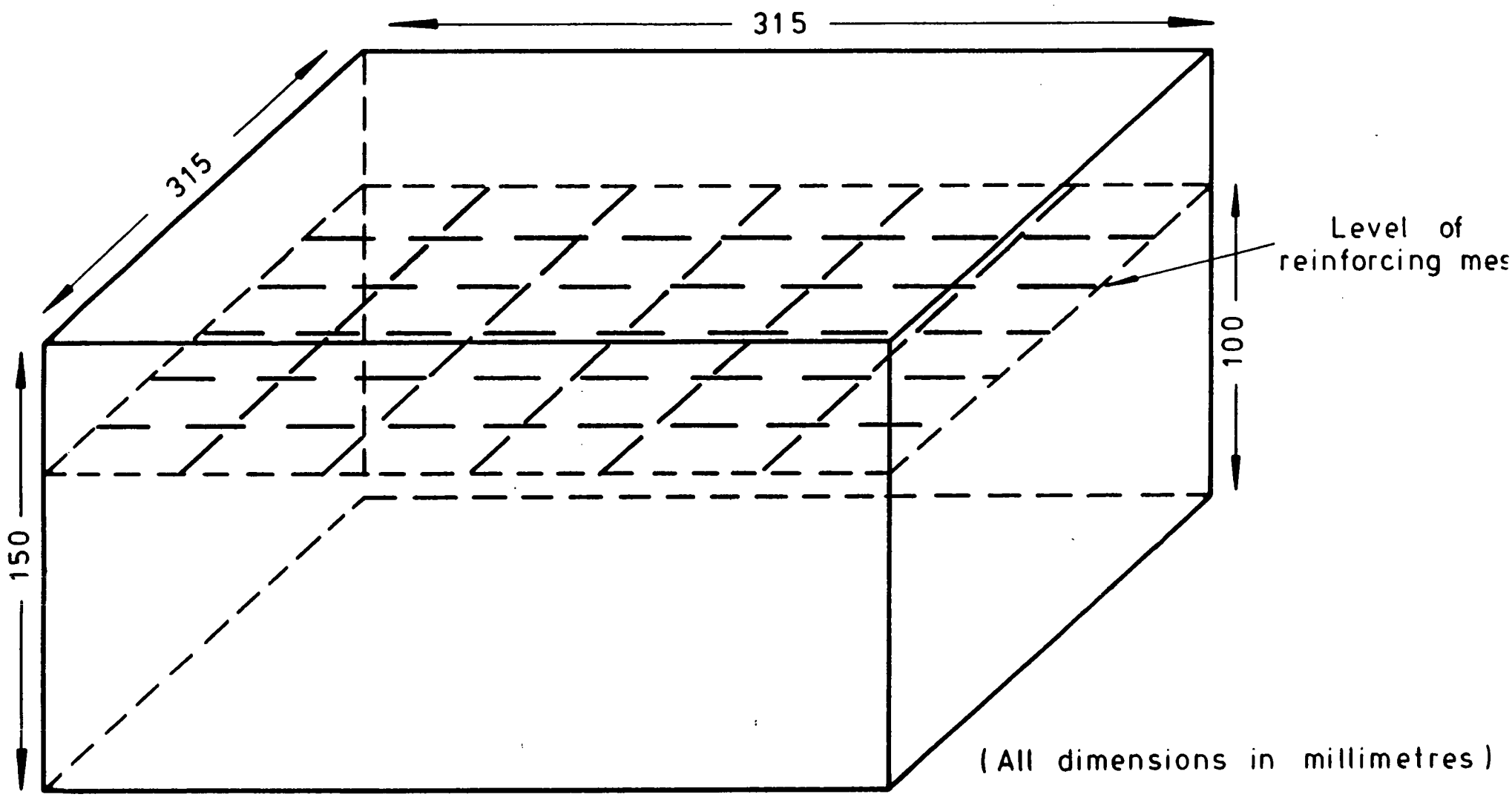

A2 2" REINFORCING MESH IN CONCRETE BLOCK.

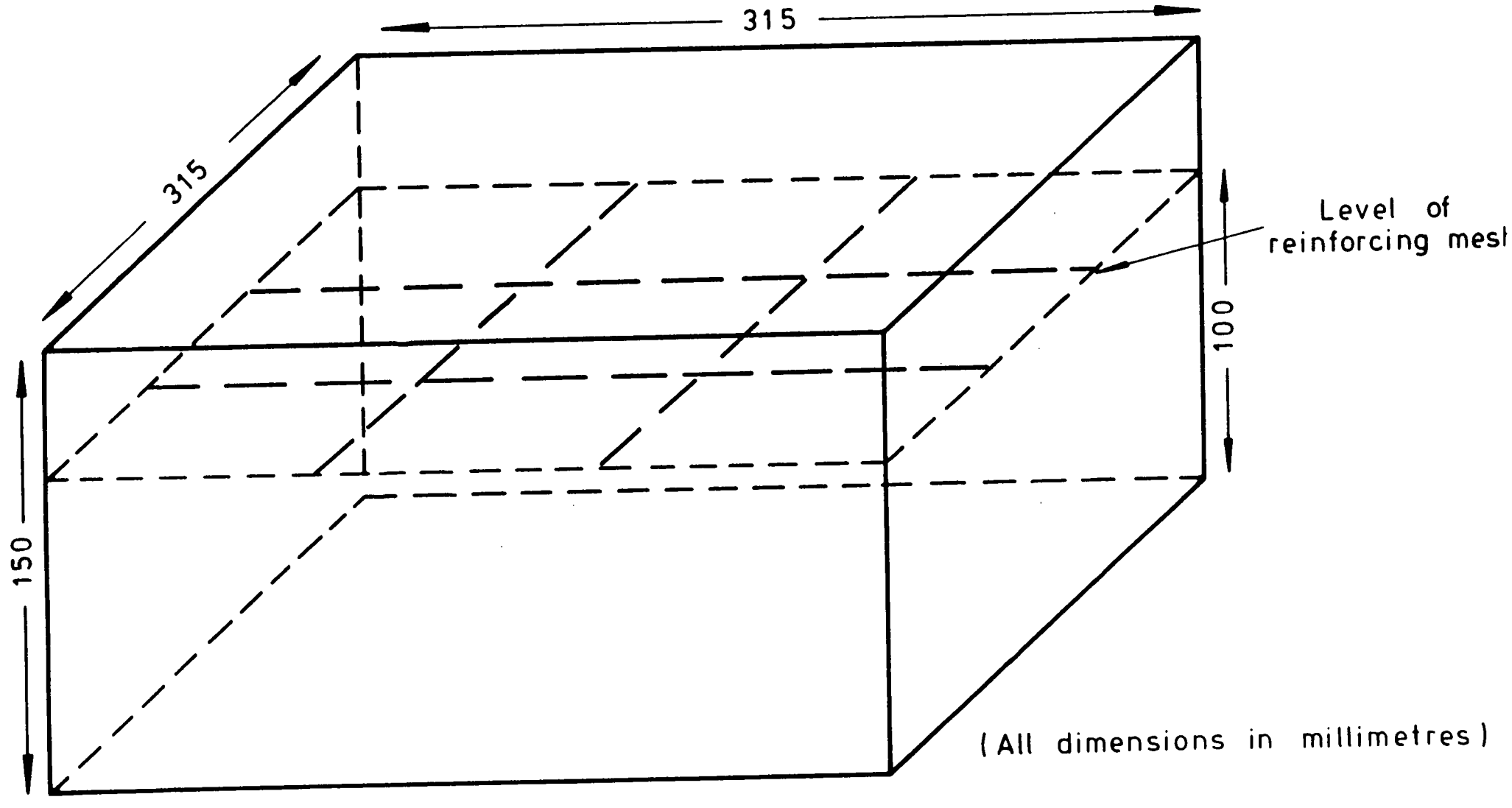

A3 4" REINFORCING MESH IN CONCRETE BLOCK.

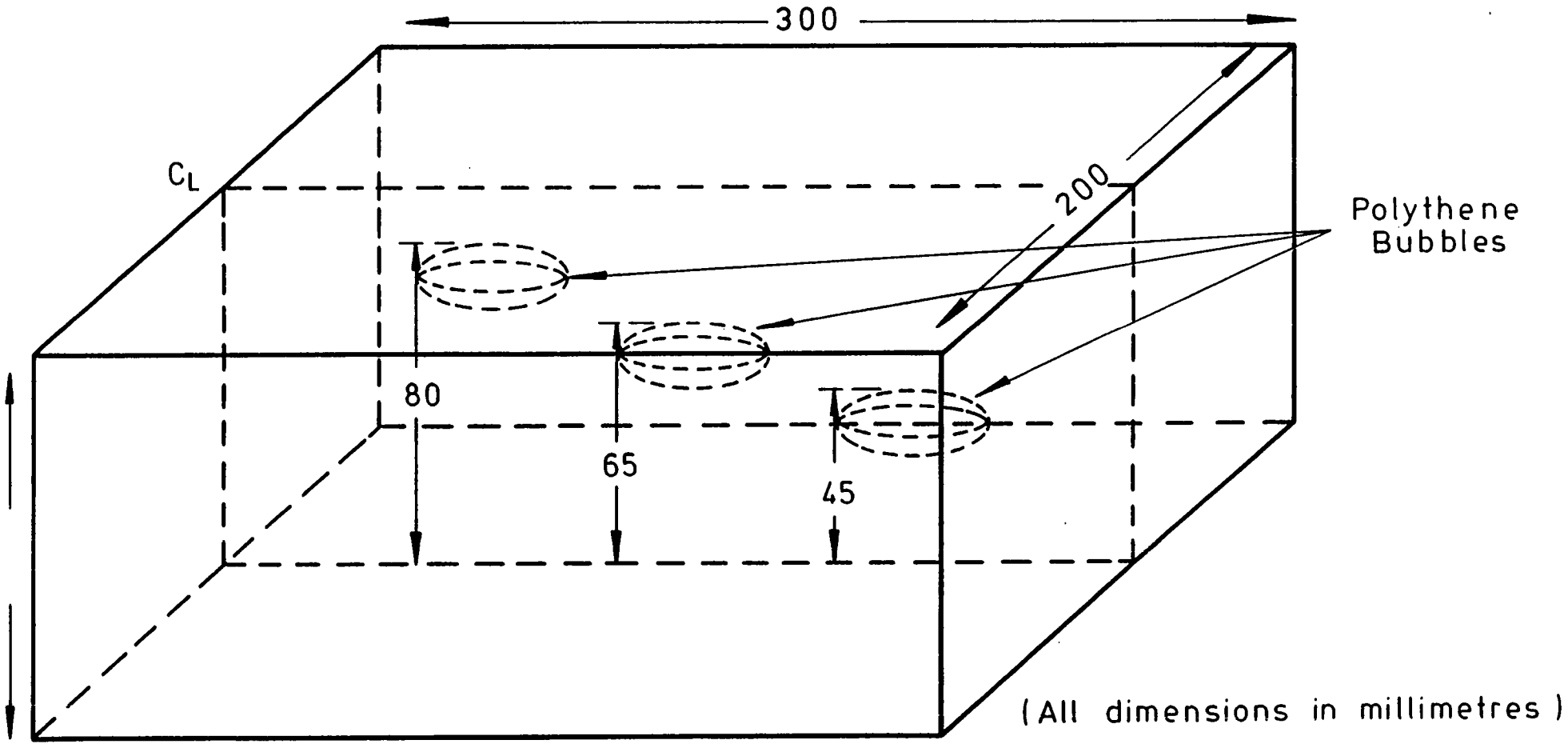

A4 TRIPLE VOID CONCRETE SAMPLE.

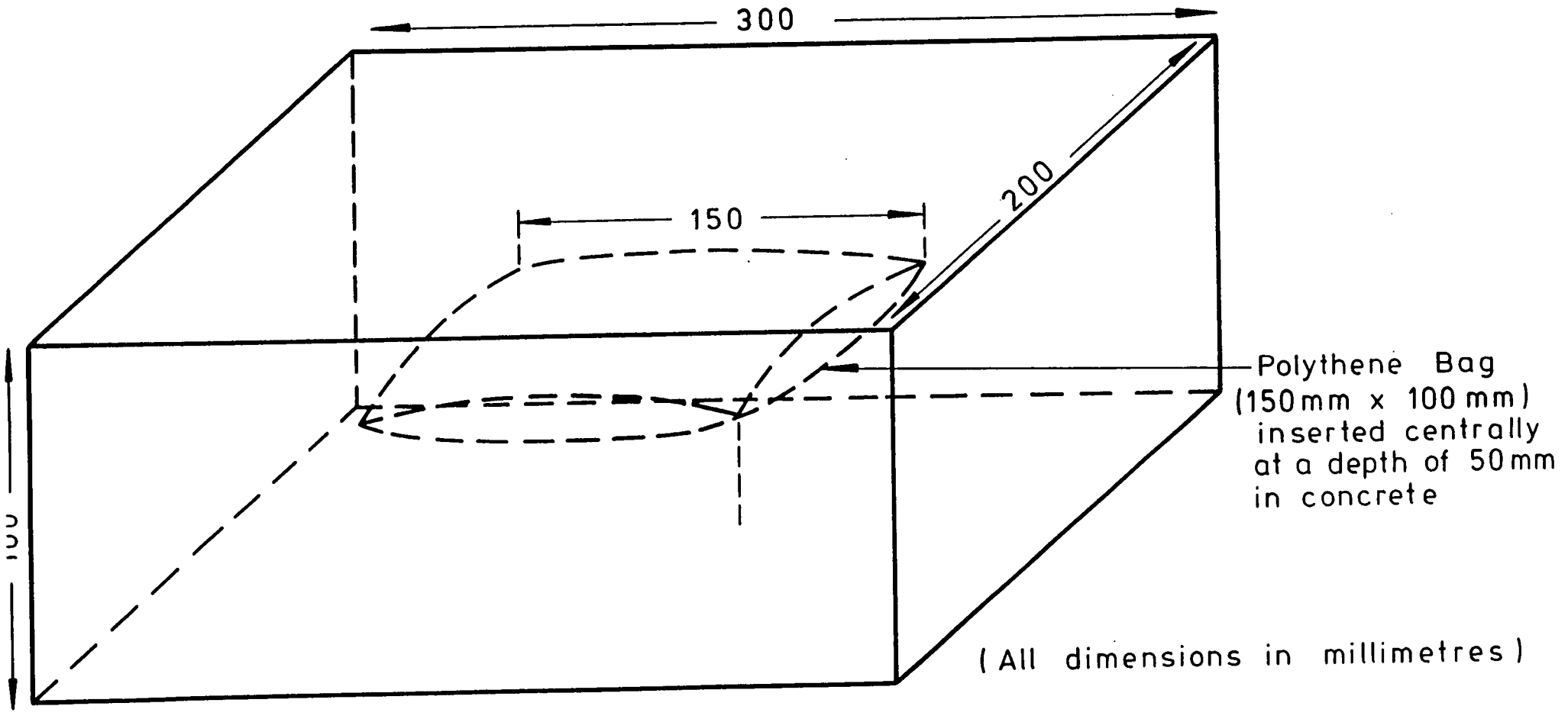

A5 SIMULATED LARGE VOID IN CONCRETE BLOCK.

Appendix B

1. Ultrasonic waves

When sound waves travel through a material, there is no actual progressive motion of the particles of the material away from the source of the sound since the motion of these particles is entirely vibrational about a fixed position. The energy from the source however is transmitted in a progressive manner and it is the arrival of this energy at a surface, and the resulting disturbance that we detect. The receiver may be a piezoelectric transducer or a laser interferometer as in this experimental work.

a) Longitudinal waves (compression waves)

Longitudinal waves (like speech) consist of alternate compressive or dilational vibrations which move in the same direction as the energy of propagation, and the vibrations of the particles will therefore be in the direction of the wave motion (Fig. B1a). The particle mechanism depends on the elastic interconnections; as each particle moves from its position of equilibrium, it pushes or pulls the adjacent particle and transmits the vibration at the velocity of sound.

b) Transverse waves (or shear waves)

It is also possible for the particles in the material to vibrate in a direction which is perpendicular to the direction of propagation of the sound, as shown in Fig. B1b. (This schematic does not indicate the actual directionality of the shear wave lobes as generated by laser impact.) These waves are called transverse waves or shear waves. Transverse waves can travel only through solids or extremely viscous 'semi-liquids' - not through normal liquids or gases because these cannot sustain shear stress. The velocity with which the shear wavefront propagates through the material is approximately 0.62 that of the compression wave velocity in

the same material. The positions of the two wavefronts in Figures B1a and B1b are equivalent for the same time-lapse.

c) Surface waves (or Rayleigh waves)

Surface waves are the result of particle motions of an elliptical or orbital nature, due to the combination of the displacements caused by a longitudinal wave component and a 90° phase-shifted shear wave component. The surface wave travels with a velocity of approximately 0.55 that of the compression wave velocity in concrete. As shown in Fig. B2a, the arrows representing the polarization vector (displacement) describe ellipses, and the wavefront propagates along the surface of the material radially from the source position. This elliptical motion of the particles ceases to be detectable at a depth equivalent to approximately one and a half wavelengths below the surface. Figure B2b is a two-dimensional schematic diagram representing what is happening to the particles in the material at any instant during the Rayleigh wave propagation along the surface.

2. Acoustic waves

These are sound waves in the audible range (such as speech) which can be propagated through air by the air molecules passing energy to each other in the same manner as compression waves. During the laser trials referred to in this report, acoustic waves - produced by the intense energy of the Nd-YAG laser pulse vaporising the material and heating the air at the impact point - were detected by the interferometer. These acoustic shock waves travel at the speed of sound in air, approximately 0.34 mm/μsec, roughly a tenth of the value of the compression wave velocity in the concrete samples used in these trials. An unfortunate aspect of the acoustic wave is that being so large, it can mask the presence of the compression wave (or shear wave) if their arrival times coincide.

3. Abbreviations used for Compression, Shear and Rayleigh waves

Throughout this report, reference has been made to P, 2P, S, 2S and R-waves; the peak positions on the waveforms corresponding to the arrival times of the compression, shear and Rayleigh waves are denoted by these abbreviations. These abbreviations are used in ultrasonics conveniently to refer to the compression wave (P-wave), the shear wave (S-wave), the 1st reflected compression wave (2P-wave), the 1st reflected shear wave (2S-wave) and the surface wave or Rayleigh wave (R-wave) as illustrated in Figures B3(a) and (b). There are also further multiples of these waves (3P, 3S, 4P and 4S), and reflected combinations are possible such as PS and SP due to 'mode conversion' where the compression wave changes into a shear wave upon reflection (from a surface or delamination), and vice versa. Although there are peaks in the waveforms due to these combinations, annotation of the waveforms has been restricted to identifying only the principal waves (R,P,S,2P and 2S).

4. Calculation of wavefront arrivals (peak positions on waveforms)

The main calculations performed to identify peaks were for the arrival times of the surface wave, the P-wave, 2P-wave, S-wave and 2S-wave and the Acoustic wave. These calculations for the 'Direct Transmission' and 'Same Surface-Separation' methods required the following values to be known: the compression wave and surface wave velocities 'V_P' and 'V_R' for the sample material, the distance of separation 'ℓ' between the two laser beams in the 'Same Surface-Separation' tests, the thickness 'd' of the sample, and the velocity of the Acoustic wave 'V_A' (0.34 mm/μsec).

In practice, V_P was found by measurement in the laboratory using the direct transmission method with two standard 50 kHz piezoelectric transducers placed on opposite faces of the concrete samples, as detailed in reference (4).

Since the surface wave is composed of components of the accompanying compression and shear waves, its velocity is related to the compression wave (and shear wave) velocity for that material by the ratio $V_R/V_P \approx 0.55$. The values of 'd' and 'ℓ' were obtained by simple measurement.

a) Notation

The following symbols are used in the calculations:

V_P - Compression wave velocity in the sample (concrete or asphalt).

V_S - Shear wave velocity in the sample.

V_R - Surface wave velocity.

V_A - Acoustic wave velocity (0.34 mm/μsec).

T_P - Arrival time of P-wave after the Nd-YAG laser pulse firing.

T_S - Arrival time of S-wave after the Nd-YAG laser pulse firing.

T_{2P}- Arrival time of 2P-wave after the Nd-YAG laser pulse firing.

T_{2S}- Arrival time of 2S-wave after the Nd-YAG laser pulse firing.

T_R - Arrival time of Surface wave after the Nd-YAG laser pulse firing.

T_A - Arrival time of Acoustic wave after the Nd-YAG laser pulse firing.

ℓ - Separation distance between the laser source beam and interferometer beam

d - Thickness or depth of sample (concrete or asphalt)

b) Calculations

(i) Direct Transmission

Time of arrival of compression wave, $T_P = \frac{d}{V_P}$ (μsec) ...(1)

Time of arrival of shear wave, $T_S = \frac{d}{V_S}$ (μsec) ...(2)

(ii) Same Surface-Separated

If the separation 'ℓ' between the two laser beams is very small compared with the thickness 'd' of the sample then:

Time of arrival of the 2P-wave, $T_{2P} = \frac{2d}{V_P}$ (μsec) ...(3)

Time of arrival of the 2S-wave, $T_{2S} = \frac{2d}{V_S}$ (μsec) ...(4)

Time of arrival of the surface wave, $T_R = \frac{\ell}{V_R}$ (μsec)

where $V_R = 0.55\ V_P$ ...(5)

Time of arrival of the Acoustic wave, $T_A = \frac{\ell}{V_A} = \frac{\ell}{0.34}$ (μsec) ..(6)

However, if 'ℓ' is not small compared with 'd', then the calculation of arrival time of the 2P-wave becomes slightly more complex and the total path length of the wavefront has to be calculated using the Pythagoras theorem, then:

Time of arrival of the 2P-wave, $T_{2P} = \frac{2(d^2+(\ell/2)^2)^{1/2}}{V_P}$ ...(7)

Similarly for the 2S-wave, $T_{2S} = \frac{2(d^2+(\ell/2)^2)^{1/2}}{V_S}$ ...(8)

In actual practice, if it were required to estimate the pavement depth, then from a waveform trace, the surface wave velocity V_R could be obtained from knowing the separation distance 'ℓ' and the surface wave arrival time T_R. From V_R a check on the position of the 2P-wave arrival peak in the waveform can be made. This will give a value for V_P and T_{2P} and hence the depth or thickness can be calculated from the expression:

$$d = 1/2 \ (V^2_P.T^2_{2P} - \ell^2)^{1/2} \qquad \ldots(9)$$

$$\text{where } V_P = \frac{\ell}{0.55\ T_R} \qquad \ldots(10)$$

(iii) Coincidence with Acoustic wave arrival

The mathematical condition to ensure that the compression wave arrival comes before the acoustic wave arrival on the waveform output is given by the expression:

$$\frac{\ell}{V_A} >> \frac{2(d^2+(\ell/2)^2)^{1/2}}{V_P} \quad (\text{ie } T_A >> T_{2P}) \qquad \ldots(11)$$

since V_A = 0.34 mm/μsec:

$$\ell >> \frac{0.68(d^2+(\ell/2)^{1/2}}{V_P} \qquad \ldots(12)$$

and in the special case of V_P = 3.4 mm/μsec then the expression becomes:

$$\ell >> \frac{(d^2+(\ell/2)^2)^{1/2}}{5} \qquad \ldots(13)$$

or as a rough guide: $\ell >> \frac{d}{5}$ $\qquad \ldots(14)$

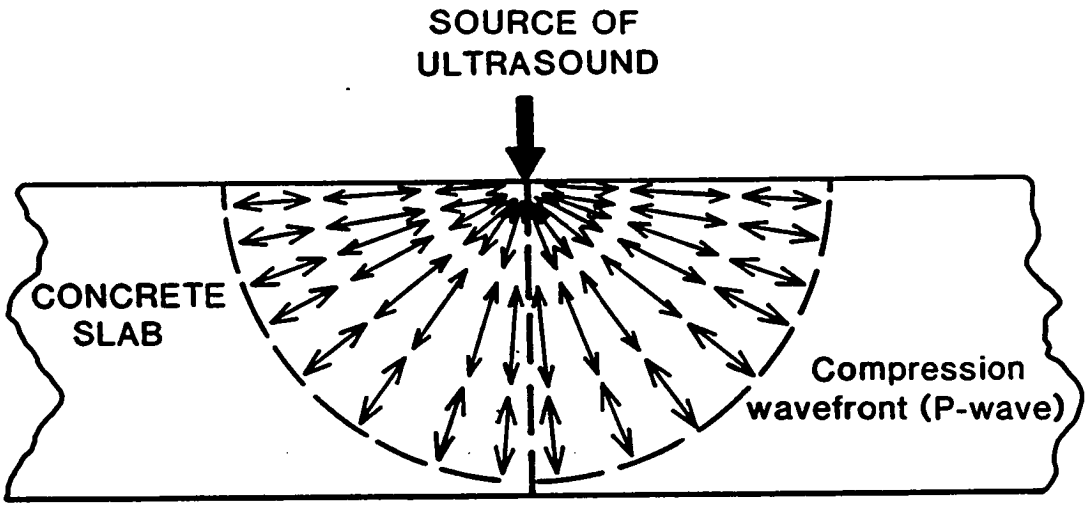

FIGURE B1 (a) Compression wave propagation with the particle vibrations in the same direction as the progression of the wavefront.

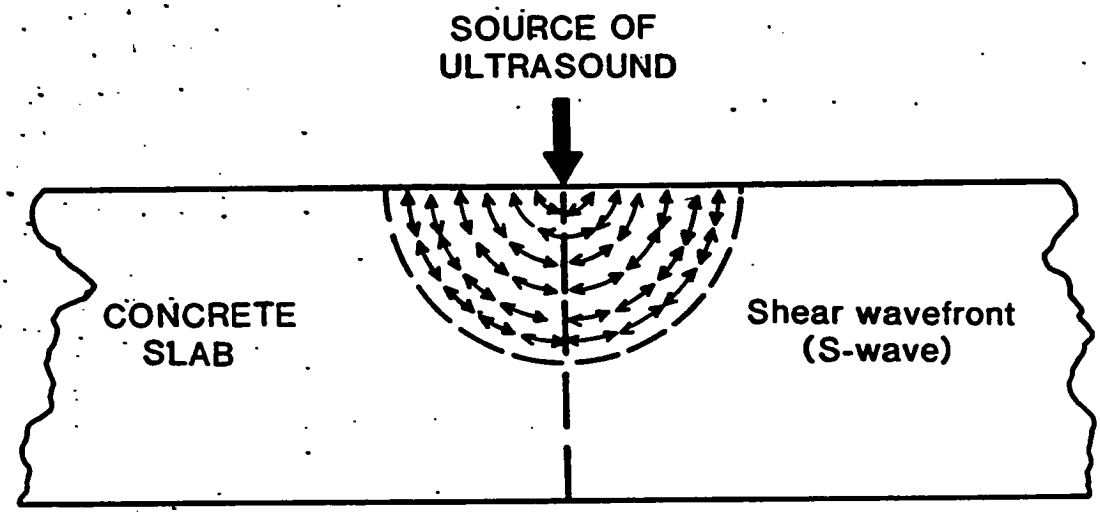

FIGURE B1 (b) Shear wave propagation with the particle vibrations perpendicular to the direction of the progression of the wavefront.

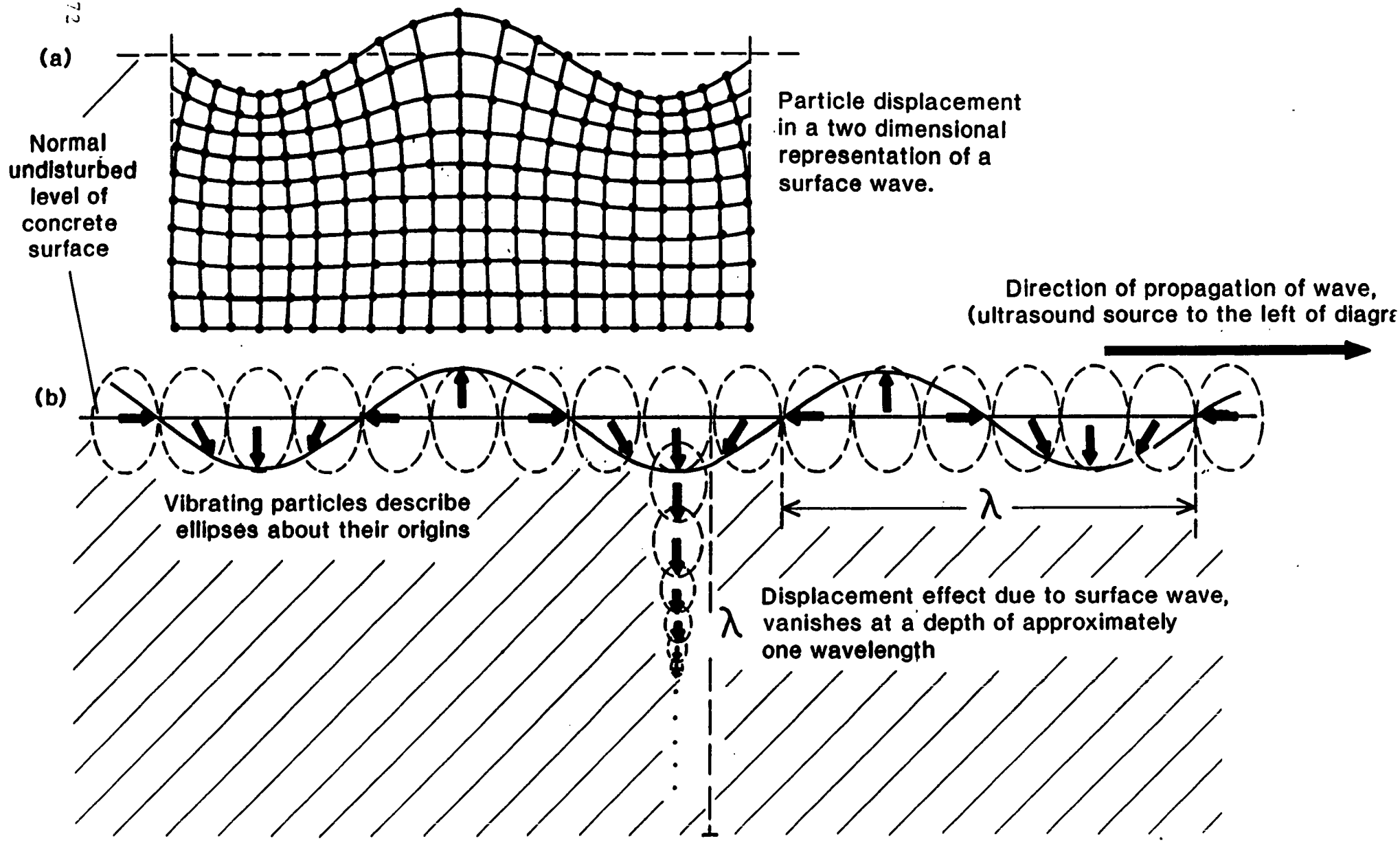

FIGURE B2 Surface wave propagation, (a) Schematic of particle displacement in one plane. (b) Polar vectors describe ellipses showing the magnitude and direction of the particle displacement along the surface.

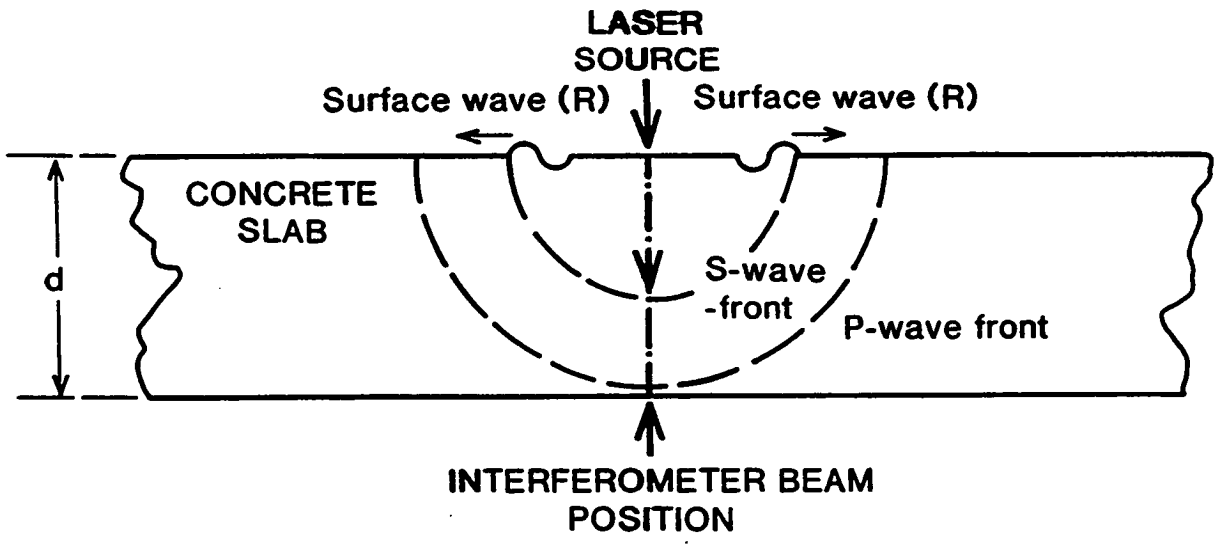

FIGURE B3(a) "DIRECT" method with laser interferometer at epicentre on opposite surface of sample from laser source. The arrival of the P-wave is about to be detected by the interferometer.

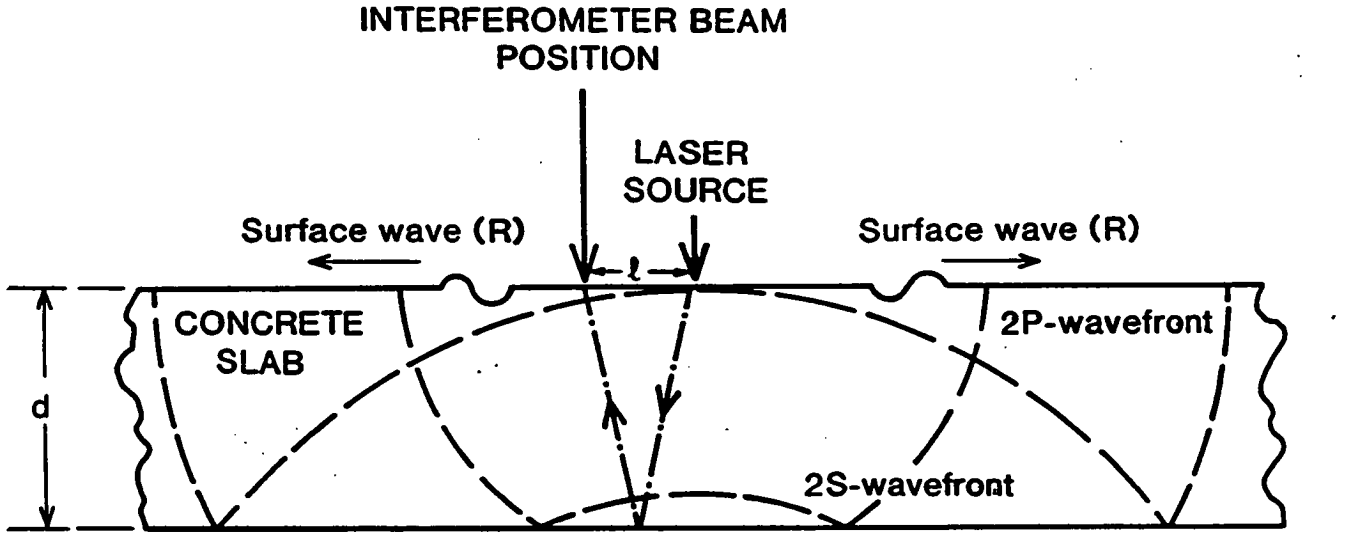

FIGURE B3(b) "SAME-SURFACE" separation method with laser interferometer on the same surface as the laser source but separated by a distance 'ℓ'. The arrival of the 2P-wave (ie.the reflected P-wave) is about to be detected by the interferometer.

The dash-dotted line shows the path taken by the ultrasound in travelling from the source to the detector in each case.

Appendix C

1. Signal to noise considerations

a) Intrinsic detector noise

As stated previously in the report, noise depends on the amount of light detected by the interferometer. Thus for the calibration voltage (which indicates amount of light) of 0.9 Volt the root mean square value of noise is 15 picometres, for 0.7 Volt the root mean square value of noise is typically twice this.

b) Acoustic noise

Due to the nature of the material, ultrasound is scattered off the aggregate, sometimes randomly, sometimes with a ringing effect following a strong pulse. In either case this resulting acoustic noise may well obscure the presence of a reflected compression wave. This problem will be existent with any ultrasonic technique but the structure of concrete and asphalt makes it particularly bad.

c) Signal strength

Signal strength was found to vary considerably and unpredictably on all samples. Normally a surface wave was easily observable but reflected compression waves and shear waves were generally much weaker except on the aged asphalt where the reflected compression wave was more prominent than the surface wave (see Figs 21 - 24).

d) Signal averaging

Signal averaging was employed to improve the signal to noise ratio. If 'n' averages (ie n laser pulses) per run are taken it reduces the genuinely random noise by the square root of 'n'. Generally 100 or 200 averages were used reducing the random noise by a factor of 10 or so.

e) Spatial averaging

In theory spatial averaging should help remove the coherent acoustic noise. This depends on the exact distribution of scatterers (aggregate) between ultrasonic generator and detector. Therefore moving the positions of the detector and generator relative to the aggregate scatterers should average out the effect of coherent acoustic noise, when each run is added together, again by a factor dependent upon the square root of the number of different positions monitored. However, the distance by which the generator and detector are moved for each position monitored should be greater than the average diameter of aggregate in the sample, otherwise the coherent acoustic noise will not change significantly. Throughout the monitoring of all positions on the same sample, the distance of separation between the generator and detector should be kept constant for spatial averaging to be effective.

f) Signal noise

The noise levels in the waveforms collected can be considered in terms of the surface displacement in fractions of a nanometre or in picometres (10^{-12} metre). Generally the following noise levels were observed:

Detector noise varied from 10 to 20 picometres and the acoustic noise varied from this level to 100 picometres. Surface wave amplitudes went from 500 to 1500 picometres, and reflected compression waves from 50 to 1000 picometres.

The signal to noise ratio for the surface wave after signal averaging was between 25 and 150, because the surface wave signal arrived before the acoustic noise had time to 'build up' and obscure it. In the waveforms obtained from the 'fresh hot rolled' and 'aged' asphalt samples it was difficult to discern the position of the surface wave. This was because the surface wave energy was very quickly dissipated and scattered on the rough asphalt surfaces and so did not reach the detector position in many cases.

The signal to noise ratios for the reflected compression wave were between 1 and 100 and in a number of waveforms obtained, the coherent acoustic noise obscured the presence of the reflected compression wave. This is where the technique of spatial averaging should be beneficial. However, as stated in the report (under Section 5, Results and Discussion, Spatial Averaging), the results obtained from spatial averaging were not always as good as expected.

2. Considerations for Practical Application of Laser System

a) Problems:-

(i) Poor reflectivity of light back to the interferometer if a light reflective coating is not applied to the surface of the concrete or asphalt.

(ii) Occasional poor acoustic coupling of generating laser to the surface if the surface has loose material (detritus) on it or it is powdery. Excess surface water will also have a debilitating effect on the energy transferred to the concrete or asphalt.

(iii) Acoustic noise can obscure the required features in the waveform.

(iv) The present equipment used for the trials in the laboratory is neither portable nor robust.

(v) The signal obtained is sensitive to variable distance between the equipment and the surface.

(vi) A higher power laser with a faster repetition rate than the one used for the laboratory

trials will be required for field trials.

(vii) With the present system, a skilled operator is required to interpret the waveforms and analyse any problems with the equipment.

(viii) It is expected that most low frequency vibrations can be compensated for by using a mechanical feed-back loop system but there may be problems with large amplitude vibrations.

(ix) There may be problems associated with the movement of the vehicle regarding the optical alignment of the interferometer to receive 'moving' reflected short bursts of light.

b) Possible solutions

(i) The use of an interferometer with a higher power laser, designed for collecting light from rough poor reflecting surfaces such as the Fabry-Perot type interferometer.

(ii) The road surface could be swept/blow cleaned before measurements take place. A device for doing this could be attached to the same vehicle as the measuring system.

(iii) Spatial averaging or radial averaging with annular focus or scanned generating beam but using a greater number of digitally averaged runs added together than hitherto tried in the laboratory should prove beneficial.

(iv) The equipment should be ruggedised for robust use. This is by no means impossible since similar instruments are manufactured for defence work and are capable of withstanding rough treatment.

(v) The optics could be chosen to give a good depth of focus.

(vi) There are other laser systems available on the market which have higher repetition rates and give greater pulse power.

(vii) Signal processing techniques to enable automatic feature recognition, data storage and analysis are well tried and fairly common and could be customised to suit the final system so that required operator skills would be minimised.

(viii) Suitable damping could be applied to the vehicle carrying the equipment, or the equipment could be mounted on damping mats.

(ix) The problem of detecting the reflected light with the interferometer moving over the surface had not been explored.

References

(1) C B Scruby, R J Dewhurst, D A Hutchings and S B Palmer, in Res Tech in NDT, Vol 5, Ch 8, ed R S Sharpe (Academic Press) 1982.

(2) M Sansalone and N J Carino, Impact Echo: A Method for Flaw Detection in Concrete using Transient Stress Waves. U S Department of Commerce, National Bureau of Standards, Report No NBSIR 86-3452, 1986.

(3) B C Moss, The Harwell Laser Interferometer, Harwell Report AERE - R10417, 1982.

(4) British Standard Institute BS 1881 (1986) Part 203. Recommendations for measurement of velocity of ultrasonic pulses in concrete.

(5) British Standard Institute BS 4987 (1988) Part 1. Coated Macadam for Roads and other Paved Areas. Specification for constituent materials and for mixtures.